EVALUATION OF FLEXIBLE LAMINATE PRINTED CIRCUIT BOARDS UNDER WIDE TEMPERATURE CYCLING

Test Report

Richard Patterson
NASA Glenn Research Center
&
Ahmad Hammoud
QSS Group, Inc.
&
Scott Gerber
ZIN Technologies

NASA Glenn Research Center
Cleveland, Ohio

August 8, 2001

Evaluation of Flexible Laminate Printed Circuit Boards Under Wide Temperature Cycling

Background

Flexible printed circuit boards constitute one of the key technology elements required by NASA for successful development of advanced power and control systems for space applications. The boards have to be lightweight, reliable, and be able to withstand operation in harsh environments. Temperature swings, which are typically experienced in planetary exploration such as Mars, comprise one of such stresses in these missions.

In a collaborative effort between NASA GRC, LaRC, and JPL under the NASA Electronic and Packaging Program (NEPP), two different flexible printed circuit boards were designed and built by NASA LaRC. Each board had a three-layer structure of insulating material with seven serpentine-like copper traces sandwiched between them. The first printed circuit board (board #1) had only polyimide as the main insulation media, while the insulating material of the other printed circuit board (board #2) consisted of a mix of polyimide and boron nitride. These boards were delivered to NASA GRC for in-house evaluation under wide temperature cycling. Photographs of board #1 and board #2 are shown in Figures 1 and 2, respectively. It is anticipated that the results of these investigations will help to understand the effects of extreme temperature exposure on the integrity and the functionality of these boards, and thereby steps can be taken in the design and construction of reliable printed circuit boards for operation under wide temperature ranges.

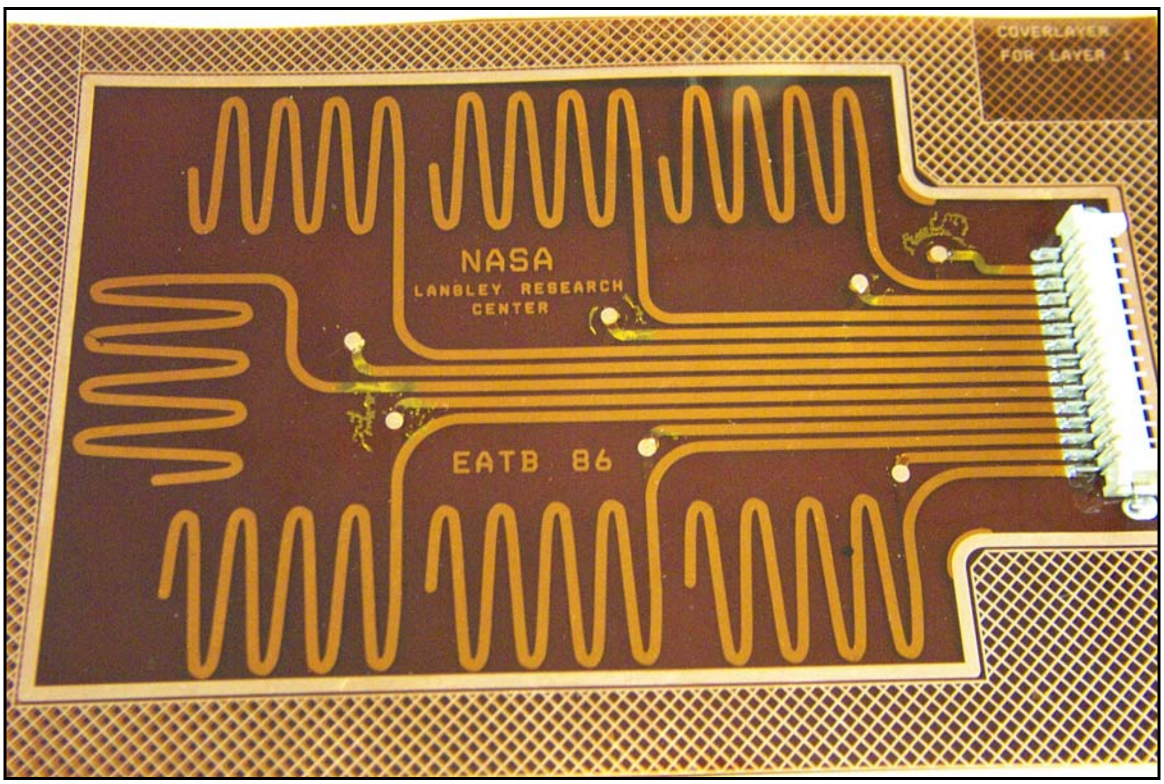

Figure 1. Photograph of Board #1.

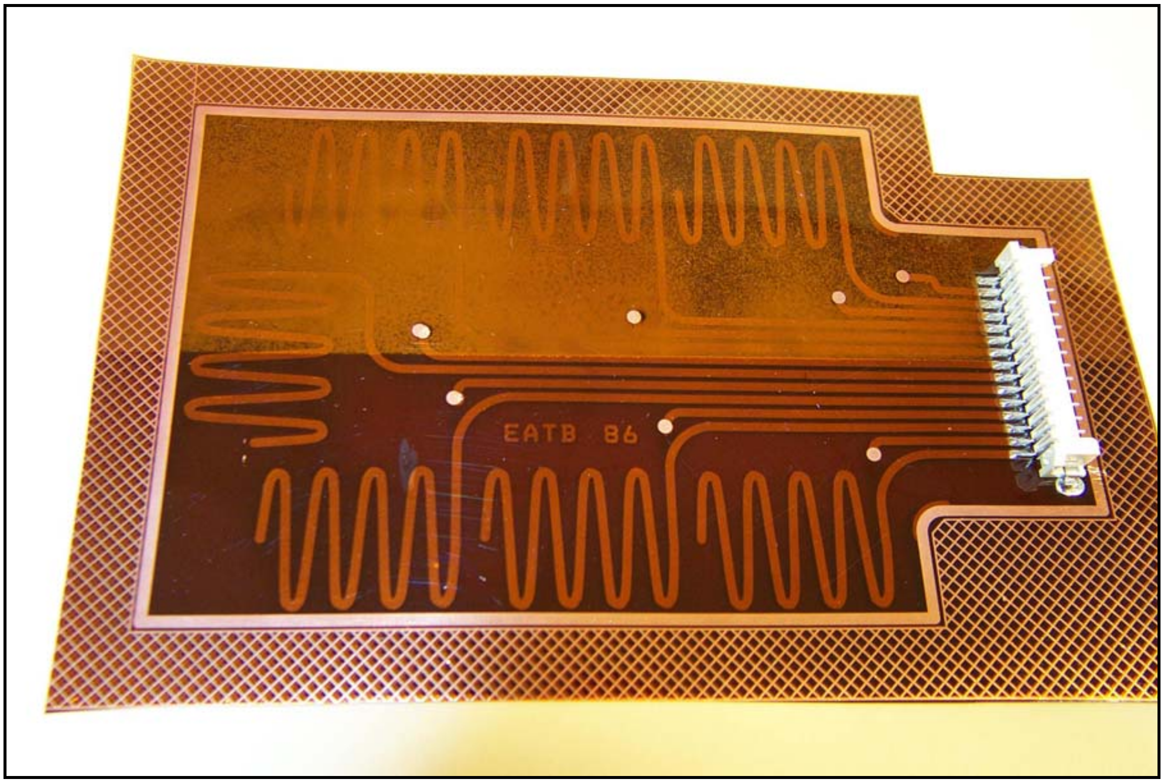

Figure 2. Photograph of Board #2.

Test Procedure and Setup

The two boards were tested separately as each was subjected to a different sequence of thermal cycling that was specified by the two NASA Centers and JPL. The thermal cycle sequence for both boards is listed in Table I. One complete thermal cycle is defined as exposing the board under test between +100 °C and –125 °C at a temperature rate of change of 10 °C/min. A soak time of 10 minutes was allowed at the extreme temperatures. Prior to any thermal cycling activity, the capacitance and dissipation factor of all seven serpentine traces of each board were measured at room temperature (pre-cycling). These dielectric properties were measured in the frequency range of 200 Hz to 500 kHz. During the first cycle, these properties were also obtained in-situ at the extreme temperatures, i.e. +100 °C and –125 °C. After completion of the first thermal cycle, the board was checked for changes in physical integrity, such as delamination, warping, discoloration; and its capacitance and dissipation factor were measured again (post-cycling). If the board under test survived the first cycle without any significant changes, then it was subjected to further cycling according to the sequence listed in Table I.

Table I. Test sequence for flexible printed circuit boards.

Board #1	Board #2
Measure capacitance & dissipation factor (pre-cycling)	Measure capacitance & dissipation factor (pre-cycling)
Do 1 cycle Measure capacitance & dissipation factor (in-situ); Measure capacitance & dissipation factor (post-cycling); Check for physical damage	Do 1 cycle Measure capacitance & dissipation factor (in-situ); Measure capacitance & dissipation factor (post-cycling); Check for physical damage
If intact; do 2 more cycles Measure capacitance (post-cycling); Check for physical damage	If intact; do 2 more cycles Measure capacitance (post-cycling); Check for physical damage
If intact; do 2 more cycles Measure capacitance (post-cycling); Check for physical damage	If intact; do 1 more cycle Measure capacitance & dissipation factor (in-situ); Measure capacitance & dissipation factor (post-cycling); Check for physical damage
If intact; do 5 more cycles Measure capacitance (post-cycling); Check for physical damage	
If intact; do 10 more cycles Measure capacitance (post-cycling); Check for physical damage	
If intact; do 1 more cycle Measure capacitance & dissipation factor (in-situ); Measure capacitance & dissipation factor (post-cycling); Check for physical damage	

Test Results of Board #1

Changes in the capacitance with temperature of the seven serpentine traces of board #1, which had only polyimide as the insulating material, during the first thermal cycle are listed in Figures 3 through 9. These results represent data taken at room temperature, as well as, at 100 °C and –125 °C. For simplicity, the capacitance values measured at only 1 kHz are reported in these figures. The investigated dielectric properties, which included both the capacitance and dissipation factor, were actually obtained in the frequency range of 200 Hz to 500 kHz. Detailed plots of these data as a function of frequency at different temperatures are given in Appendix A.

A close examination of Figure 3, which depicts capacitance of trace 1 as a function of temperature during the first cycle, shows that the capacitance exhibited an increase as temperature was increased from room temperature to 100 °C. When the test temperature was lowered to –125 °C, the capacitance decreased to a level below its room temperature value. There seems to be a somewhat linear relationship between the capacitance of the metallic trace and the temperature. For example, while the capacitance increased by about 5 % at 100 °C, it lost about 7 % of its room temperature value when measured at –125 °C. Similar to trace 1, the other six traces of board #1 have displayed almost an exact behavior in their capacitance with temperature as can be seen in Figures 4 through 9. The changes experienced in the capacitance of all seven traces with temperature seem, however, to be transitory in nature as the capacitance of each trace recovered to its respective room temperature value after thermal cycling was completed. In addition, no structural damage was incurred by the board due to this first cycle as no delamination, breakage, warping, or other physical alteration was observed.

The board was then subjected to two additional cycles followed by measurements of its dielectric properties and a full examination of its physical integrity. Once again, no permanent changes were observed in its electrical or physical characteristics. In fact, such was the case even after the additional cycling sequence (a total of 20 cycles) was completed. The pre-cycling data along with the measured results obtained in between these cycling runs for the capacitance of all seven traces are shown in Tables II, III, and IV at a frequency of 1 kHz, 10 kHz, and 100 kHz, respectively. While some variations appear in the measurements for a given trace, as listed in these tables, they are very minimal and occur infrequently. These changes are mainly attributed to the parasitic effects introduced by the wire leads that connect the flexible circuit board inside the environmental chamber to the external instrumentation. Instrument accuracy at the very low frequencies and change in the humidity level, although controlled, might have also played a factor.

At the end of the thermal cycle sequence as listed in Table I, the board was then subjected to one additional cycle and capacitance measurements of all seven serpentine traces were taken at 25 °C, 100 °C and –125 °C. The data obtained during this 21st cycle are plotted and compared to those of the first cycle in Figures 10 through 16 for trace 1 through trace 7, respectively. It can be clearly seen that each and every trace has displayed the same trend in capacitance change with temperature. It appears that this limited thermal cycling activity, a total of 21 cycles in the temperature range of 100 °C to –125 °C, produced no effect on the electrical or physical characteristics of the flexible printed circuit board #1.

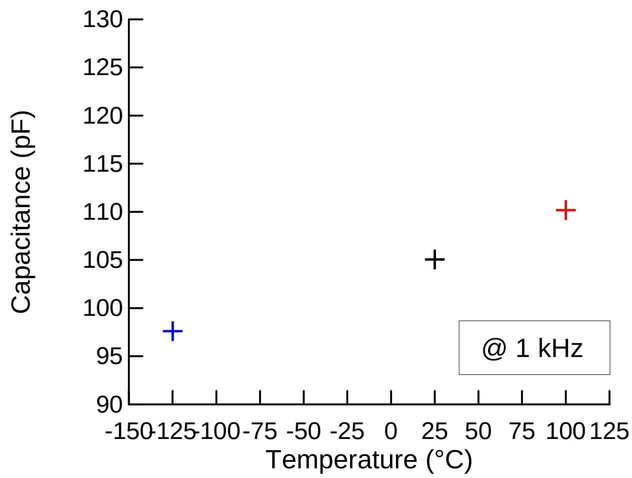

Figure 3. Capacitance versus temperature for trace 1 of board #1 @ 1 kHz.

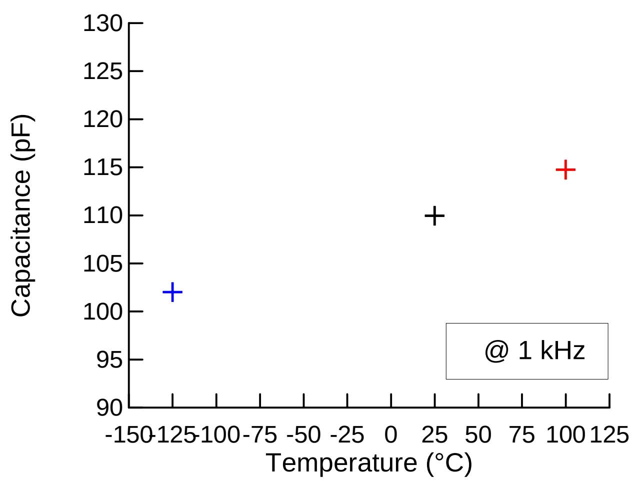

Figure 4. Capacitance versus temperature for trace 2 of board #1 @ 1 kHz.

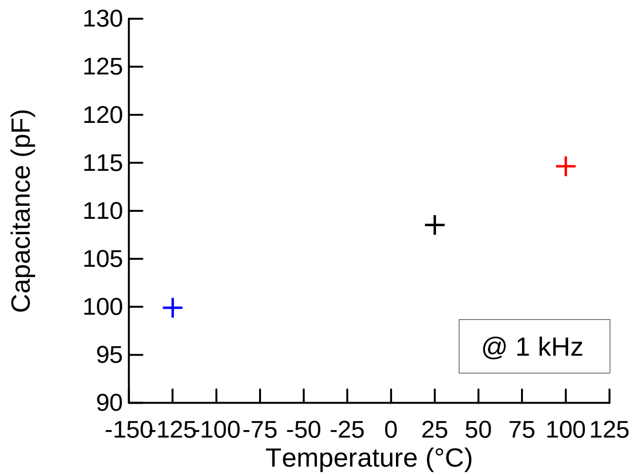

Figure 5. Capacitance versus temperature for trace 3 of board #1 @ 1 kHz.

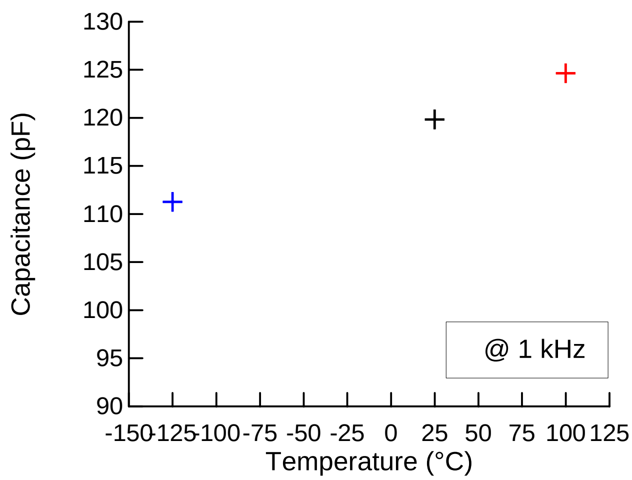

Figure 6. Capacitance versus temperature for trace 4 of board #1 @ 1 kHz.

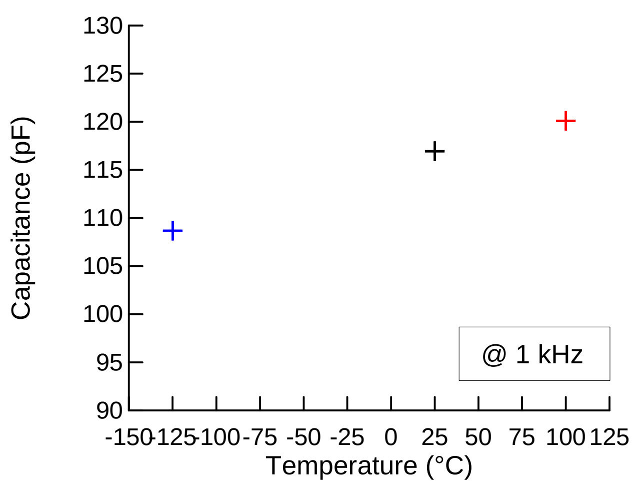

Figure 7. Capacitance versus temperature for trace 5 of board #1 @ 1 kHz.

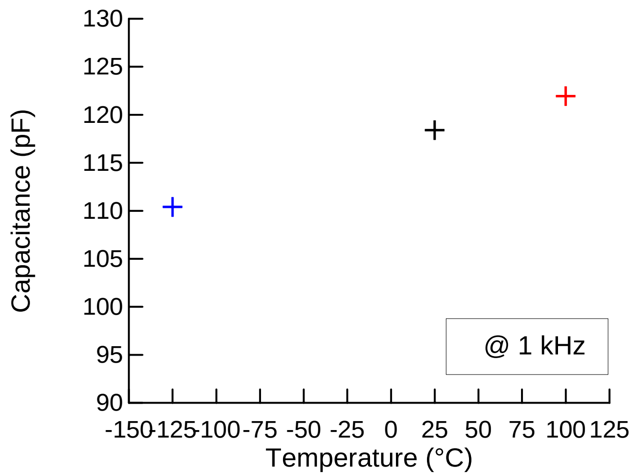

Figure 8. Capacitance versus temperature for trace 6 of board #1 @ 1 kHz.

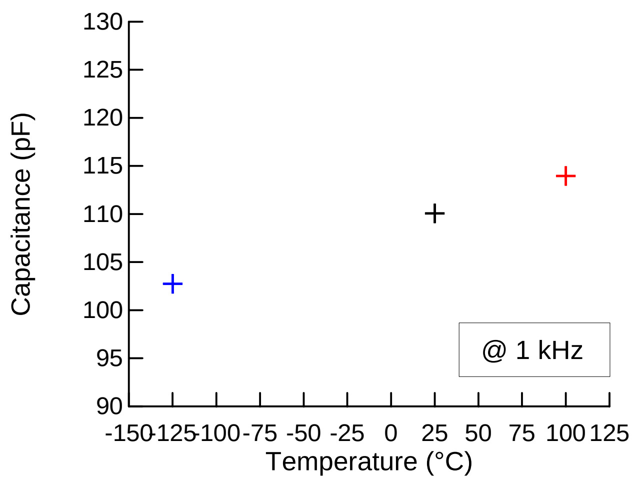

Figure 9. Capacitance versus temperature for trace 7 of board #1 @ 1 kHz.

Table II. Capacitance (pF) for board #1 at 1 kHz as a function of thermal cycling.

	original value	values after consecutive				
		1 cycle	2 cycles	2 cycles	5 cycles	10 cycles
Trace 1	105.06	104.92	104.32	105.10	103.73	105.19
Trace 2	109.94	110.30	108.82	110.15	107.03	110.19
Trace 3	108.50	108.51	107.90	108.24	106.24	108.09
Trace 4	119.83	119.69	119.04	118.94	116.95	119.48
Trace 5	116.94	117.20	117.29	115.95	114.28	115.9
Trace 6	118.39	117.78	117.39	116.70	114.58	117.07
Trace 7	110.06	109.55	109.55	108.81	106.35	109.75

Table III. Capacitance (pF) for board #1 at 10 kHz as a function of thermal cycling.

	Original value	values after consecutive				
		1 cycle	2 cycles	2 cycles	5 cycles	10 cycles
Trace 1	103.17	102.84	102.07	102.88	101.35	103.19
Trace 2	107.77	107.99	106.52	107.94	104.90	108.03
Trace 3	106.23	106.24	105.39	106.00	103.72	106.07
Trace 4	117.55	117.47	116.41	116.76	114.70	117.5
Trace 5	114.97	115.16	114.65	114.01	112.20	114.28
Trace 6	116.50	115.87	115.17	114.84	112.54	115.43
Trace 7	108.10	107.50	107.31	106.83	104.48	107.92

Table IV. Capacitance (pF) for board #1 at 100 kHz as a function of thermal cycling.

	Original value	values after consecutive				
		1 cycle	2 cycles	2 cycles	5 cycles	10 cycles
Trace 1	100.98	100.52	99.70	100.56	98.73	100.86
Trace 2	105.47	105.52	104.10	105.46	102.58	105.6
Trace 3	103.83	103.77	102.88	103.47	101.06	103.7
Trace 4	115.16	114.97	113.80	114.25	112.18	115.05
Trace 5	112.71	112.81	112.04	111.69	109.90	112.09
Trace 6	114.26	113.59	112.56	112.59	110.12	113.29
Trace 7	105.78	105.15	104.86	104.53	102.23	105.69

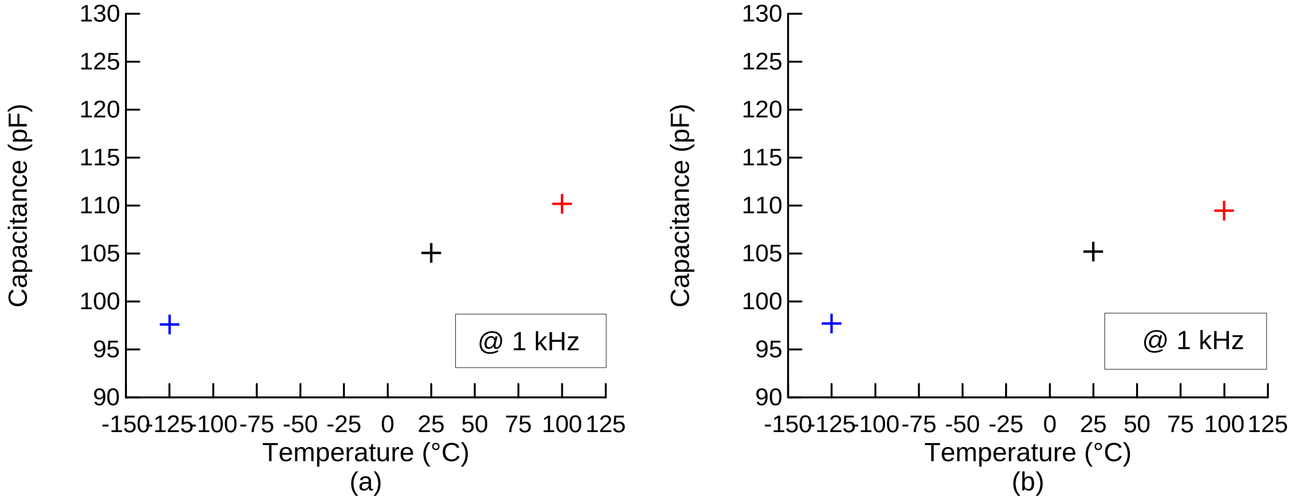

Figure 10. Capacitance versus temperature for trace 1 of board #1 during initial cycle (a), and after 21 cycles (b).

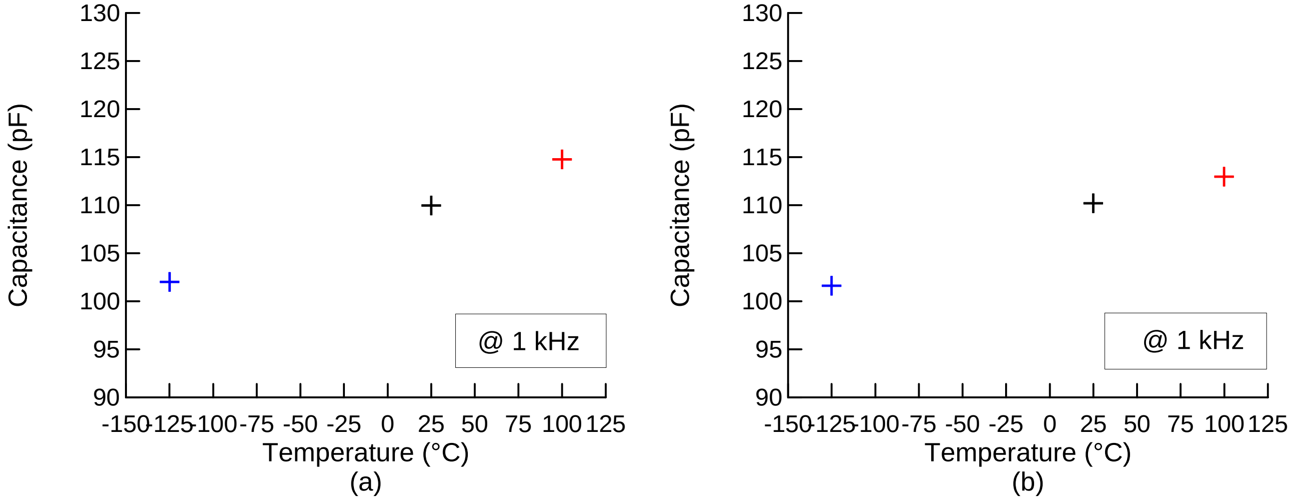

Figure 11. Capacitance versus temperature for trace 2 of board #1 during initial cycle (a), and after 21 cycles (b).

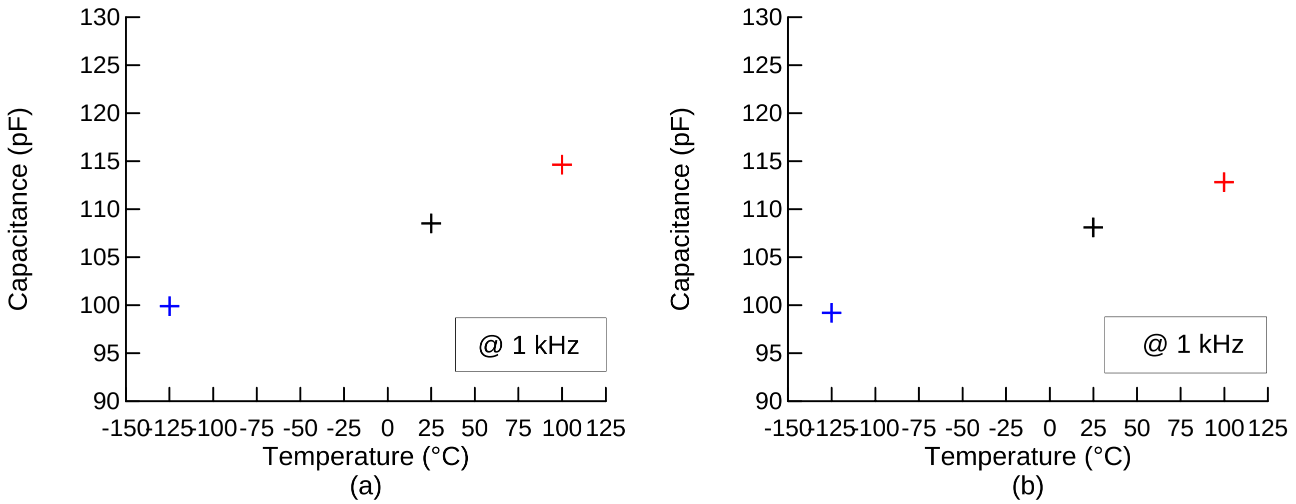

Figure 12. Capacitance versus temperature for trace 3 of board #1 during initial cycle (a), and after 21 cycles (b).

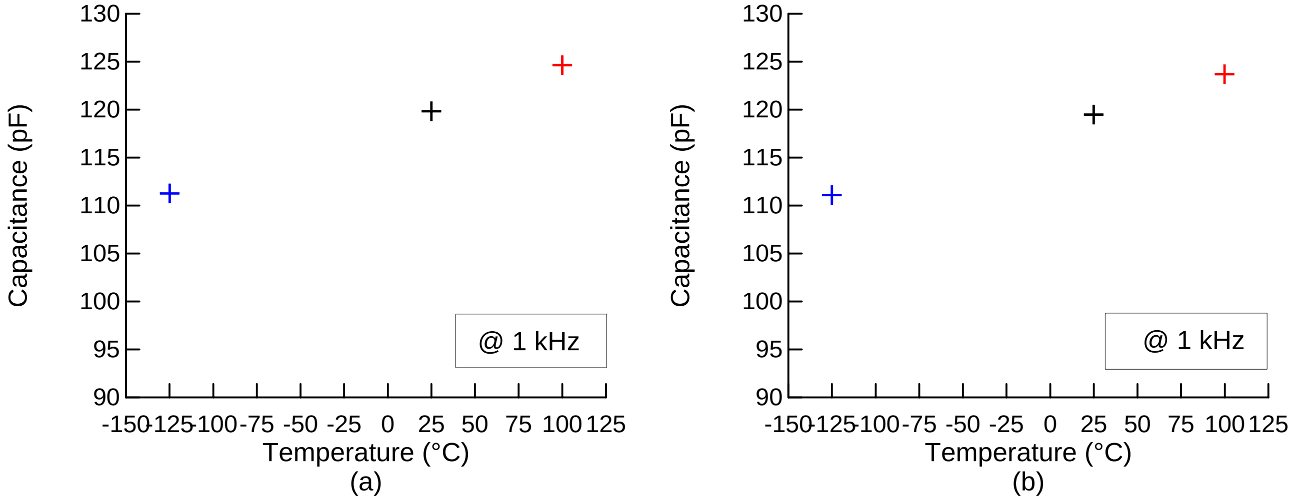

Figure 13. Capacitance versus temperature for trace 4 of board #1 during initial cycle (a), and after 21 cycles (b).

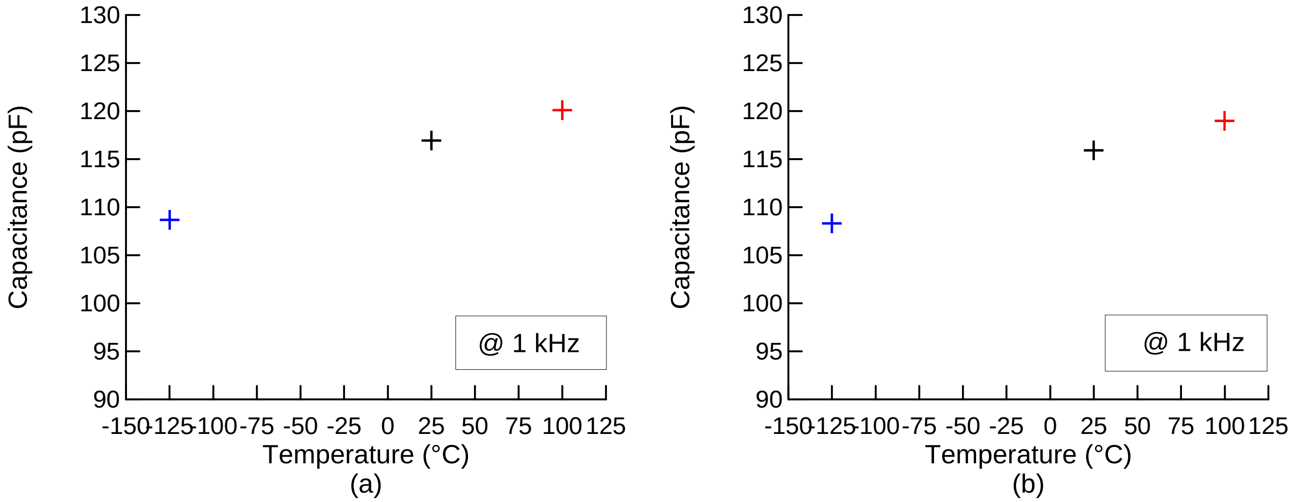

Figure 14. Capacitance versus temperature for trace 5 of board #1 during initial cycle (a), and after 21 cycles (b).

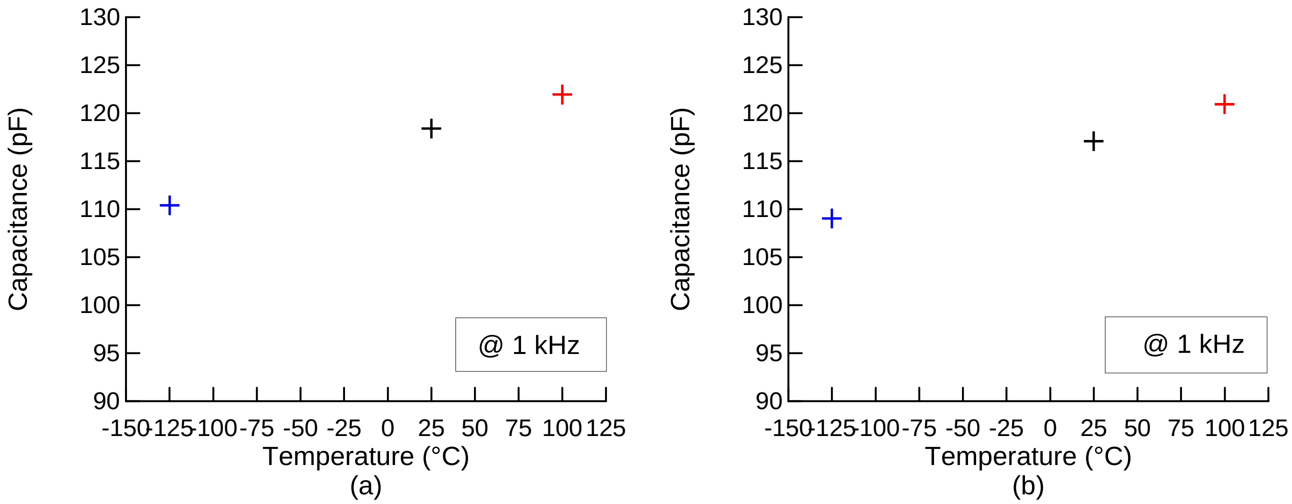

Figure 15. Capacitance versus temperature for trace 6 of board #1 during initial cycle (a), and after 21 cycles (b).

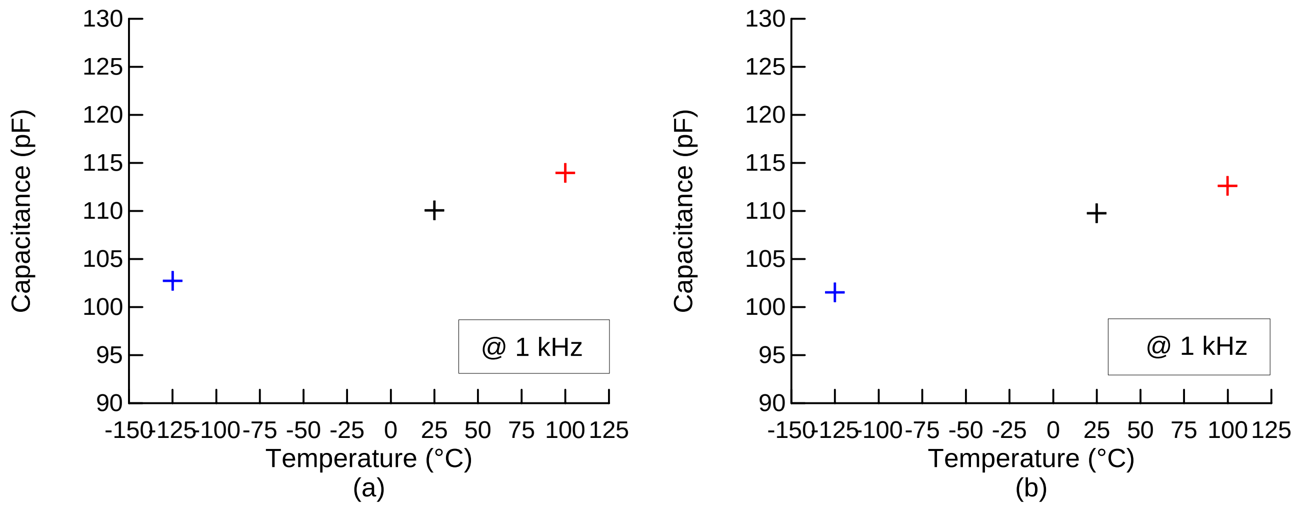

Figure 16. Capacitance versus temperature for trace 7 of board #1 during initial cycle (a), and after 21 cycles (b).

Test Results of Board #2

Changes in the capacitance with temperature of the seven serpentine traces of board #2, which had polyimide insulation with boron nitride additive, during the first thermal cycle are listed in Figures 17 through 23. These results represent data taken at room temperature, as well as, at 100 °C and –125 °C. For simplicity, the capacitance values measured at only 1 kHz are reported in these figures. As with board #1, the investigated dielectric properties were obtained in the frequency range of 200 Hz to 500 kHz. Detailed plots of these data as a function of frequency at different temperatures are also given in Appendix A.

A close examination of Figure 17, which depicts capacitance of trace 1 as a function of temperature during the first cycle, shows that the capacitance exhibited an increase of about 3% as temperature was increased from room temperature to 100 °C. When the test temperature was lowered to –125 °C, the capacitance decreased by about 8.5% of its room temperature value. Similar to board #1, there seems to be a somewhat linear relationship between the capacitance of the metallic trace and the temperature. All changes in the dielectric properties of this trace seem to be transitory in nature as they recovered to their original values after thermal cycling was completed. In addition, the board experienced no observable damage such as delamination, breakage, warping, or other physical alteration due to this first thermal cycle.

Similar to trace 1, traces 2, 3 and 4 have displayed almost an exact behavior in capacitance with temperature as can be seen in Figures 18, 19 and 20, respectively. The remaining three traces; i.e. traces 5-7, exhibited similar behavior in the dielectric properties with temperature except their capacitance characteristics at 100 °C, as shown in Figures 21 through 23. Unlike the other traces, the values of their capacitance did not undergo any appreciable increase when temperature was increased to 100 °C. It is not really understood why such a trend is observed in these traces. It is important however to point out that the section of this board comprising these traces is different from the remainder of the board containing the other traces. Upon careful examination of the board as pictured in Figure 2, this section seems to be more cloudy and opaque. These features, which were apparent on the board prior to any testing, did not undergo any changes due to thermal cycling.

Board #2 was then subjected to two additional cycles followed by full examination of its physical integrity and measurements of its capacitance. Once again, no permanent changes were observed in its electrical or physical characteristics. The pre-cycling data along with the measured results obtained after the two thermal cycling runs for the capacitance of all seven traces are shown in Tables V, VI, and VII at a frequency of 1 kHz, 10 kHz, and 100 kHz, respectively. Similar to board #1 results, some variations appear in the reported measurements, but these variations are very minimal and occur infrequently. As mentioned before, these changes are mainly attributed to the parasitic effects introduced by the wire leads, which connect the flexible circuit board inside the environmental chamber to the external instrumentation, and to instrument inaccuracy at the very low frequencies.

At the end of the thermal cycle sequence as listed in Table I, the board was then subjected to one additional cycle and capacitance measurements of all seven serpentine traces were taken at 25 °C, 100 °C and –125 °C. The data obtained during this 4th cycle are plotted and compared to those of the first cycle in Figures 24 through 30 for trace 1 through trace 7, respectively. It appears that all traces display similar trend in capacitance with temperature as before. This limited thermal cycling activity, which comprised of a total of 4 cycles in the temperature range of 100 °C to –125 °C, produced no effect on the electrical or physical characteristics of the flexible printed circuit board #2.

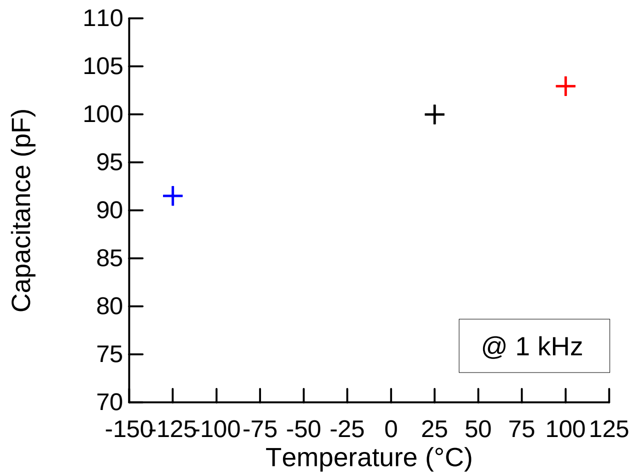

Figure 17. Capacitance versus temperature for trace 1 of board #2 @ 1 kHz.

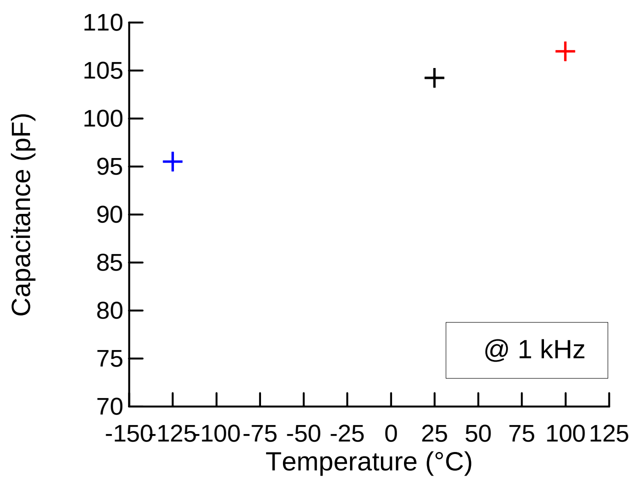

Figure 18. Capacitance versus temperature for trace 2 of board #2 @ 1 kHz.

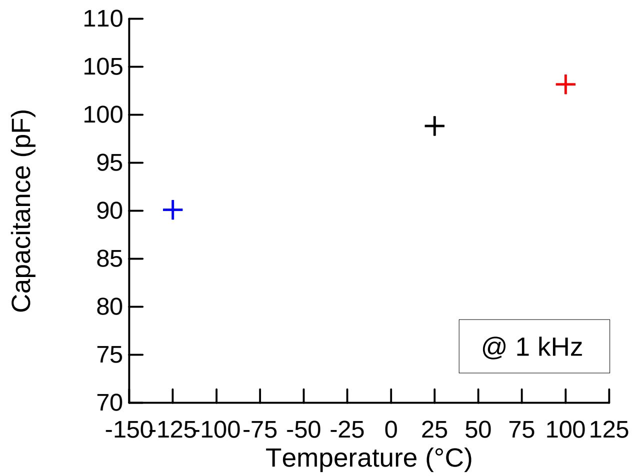

Figure 19. Capacitance versus temperature for trace 3 of board #2 @ 1 kHz.

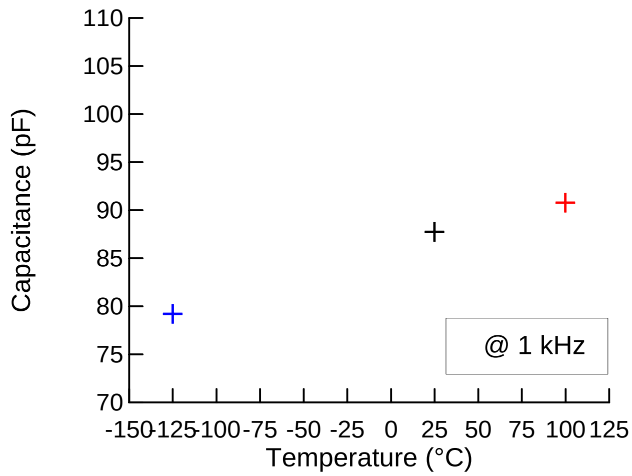

Figure 20. Capacitance versus temperature for trace 4 of board #2 @ 1 kHz.

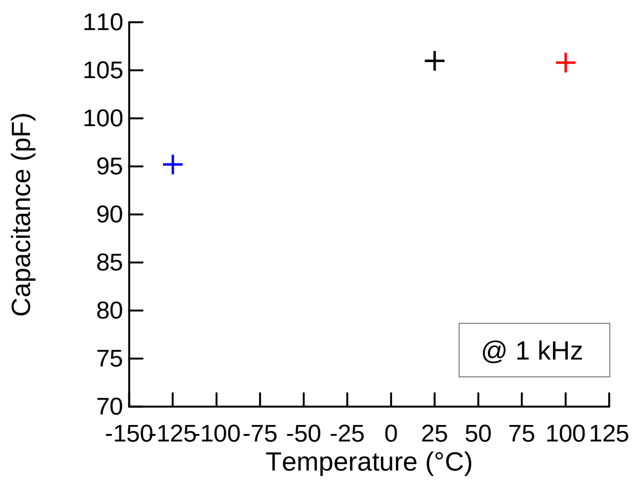

Figure 21. Capacitance versus temperature for trace 5 of board #2 @ 1 kHz.

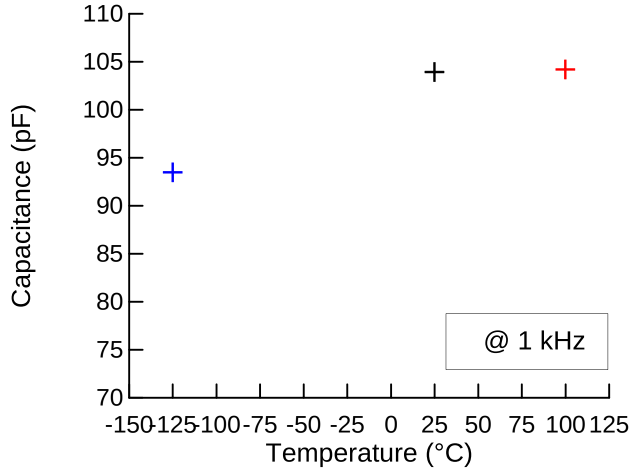

Figure 22. Capacitance versus temperature for trace 6 of board #2 @ 1 kHz.

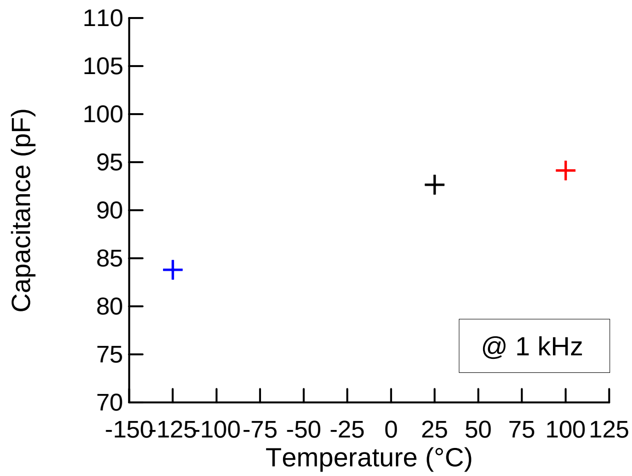

Figure 23. Capacitance versus temperature for trace 7 of board #2 @ 1 kHz.

Table V. Capacitance (pF) for board #2 at 1 kHz as a function of thermal cycling.

	original value	values after consecutive 1 cycle	2 cycles
Trace 1	99.98	100.55	99.47
Trace 2	104.24	104.59	102.08
Trace 3	98.82	99.05	96.60
Trace 4	87.74	87.90	85.81
Trace 5	105.97	107.47	102.54
Trace 6	103.93	105.39	102.15
Trace 7	92.66	93.44	91.46

Table VI. Capacitance (pF) for board #2 at 10 kHz as a function of thermal cycling.

	original value	values after consecutive 1 cycle	2 cycles
Trace 1	98.19	98.54	97.85
Trace 2	102.21	102.49	100.50
Trace 3	96.90	97.12	95.13
Trace 4	85.82	85.94	84.11
Trace 5	104.10	104.82	101.00
Trace 6	102.09	102.92	100.40
Trace 7	90.77	91.19	89.57

Table VII. Capacitance (pF) for board #2 at 100 kHz as a function of thermal cycling.

	Original value	values after consecutive 1 cycle	2 cycles
Trace 1	95.98	96.34	95.88
Trace 2	99.49	100.12	98.48
Trace 3	94.55	94.82	93.08
Trace 4	83.54	83.71	82.03
Trace 5	101.80	102.15	98.99
Trace 6	99.87	100.40	98.23
Trace 7	88.56	88.87	87.38

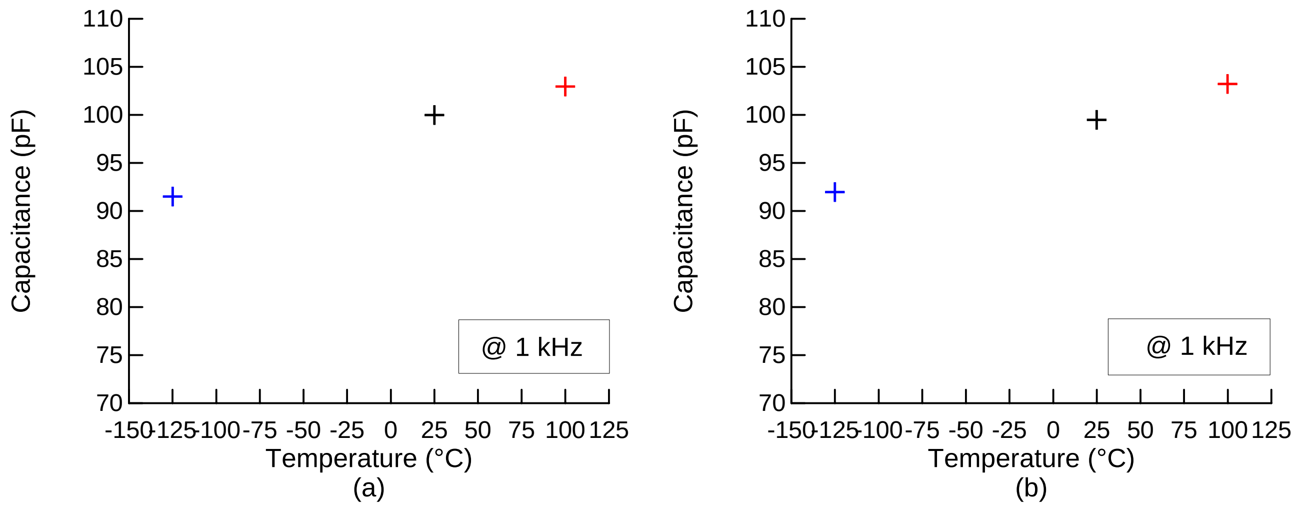

Figure 24. Capacitance versus temperature for trace 1 of board #2 during initial cycle (a), and after 4 cycles (b).

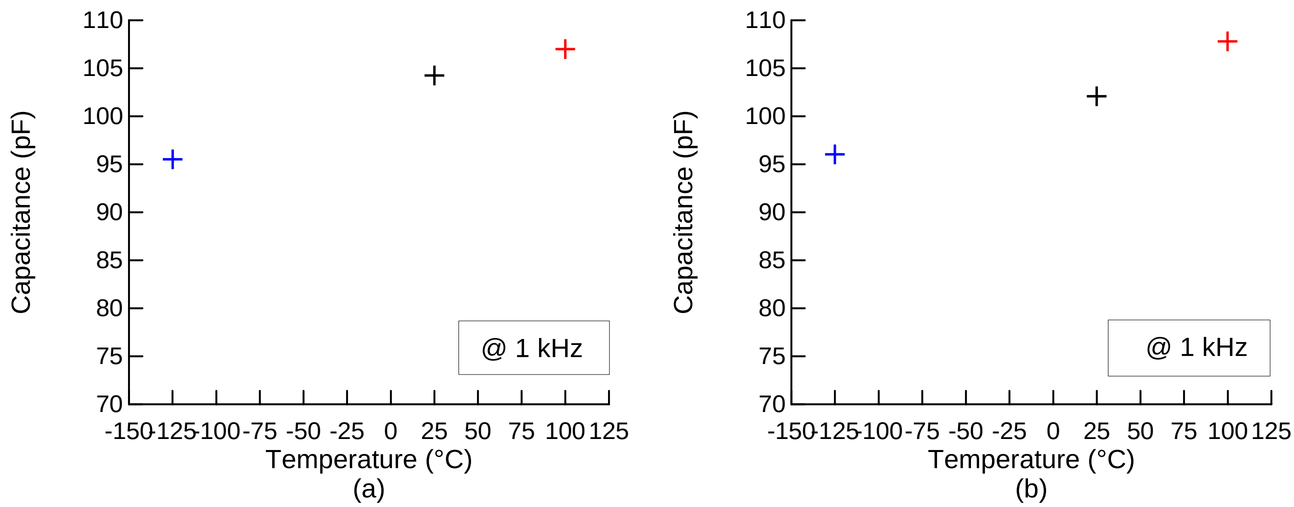

Figure 25. Capacitance versus temperature for trace 2 of board #2 during initial cycle (a), and after 4 cycles (b).

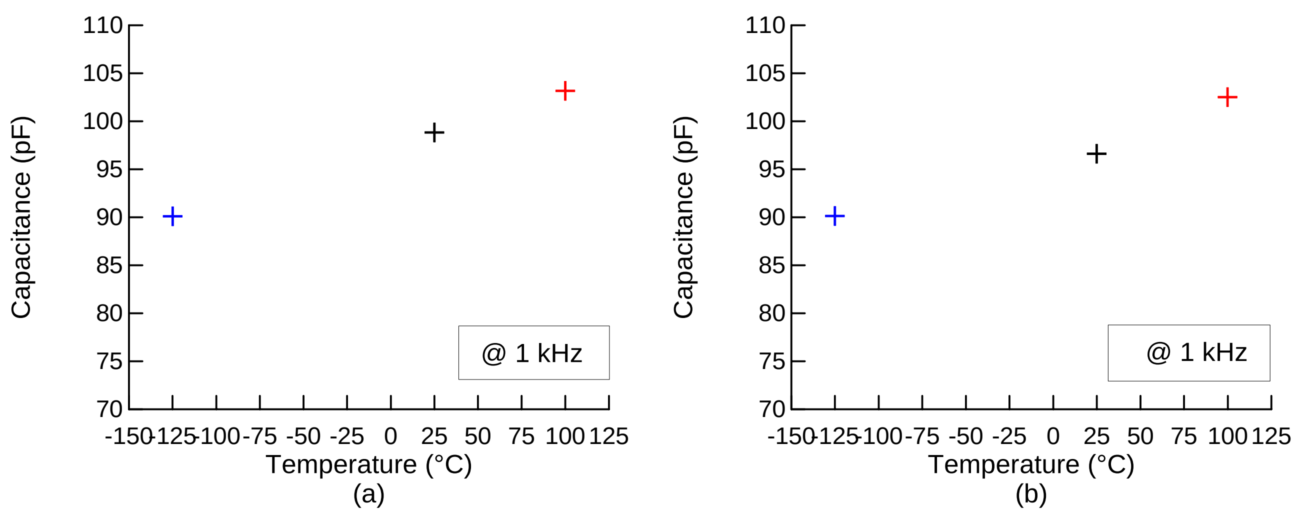

Figure 26. Capacitance versus temperature for trace 3 of board #2 during initial cycle (a), and after 4 cycles (b).

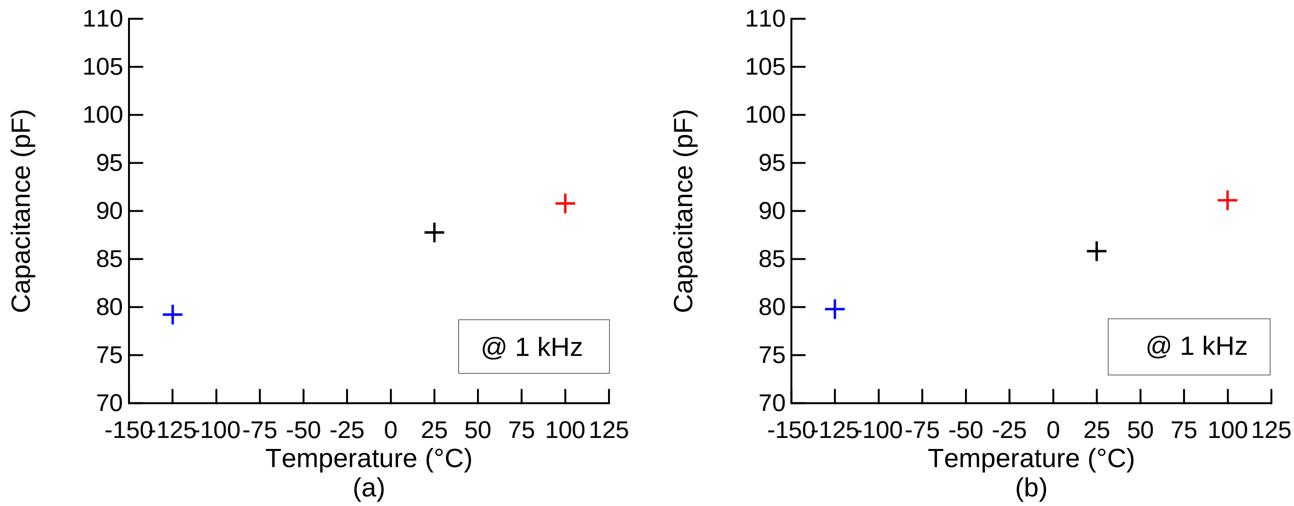

Figure 27. Capacitance versus temperature for trace 4 of board #2 during initial cycle (a), and after 4 cycles (b).

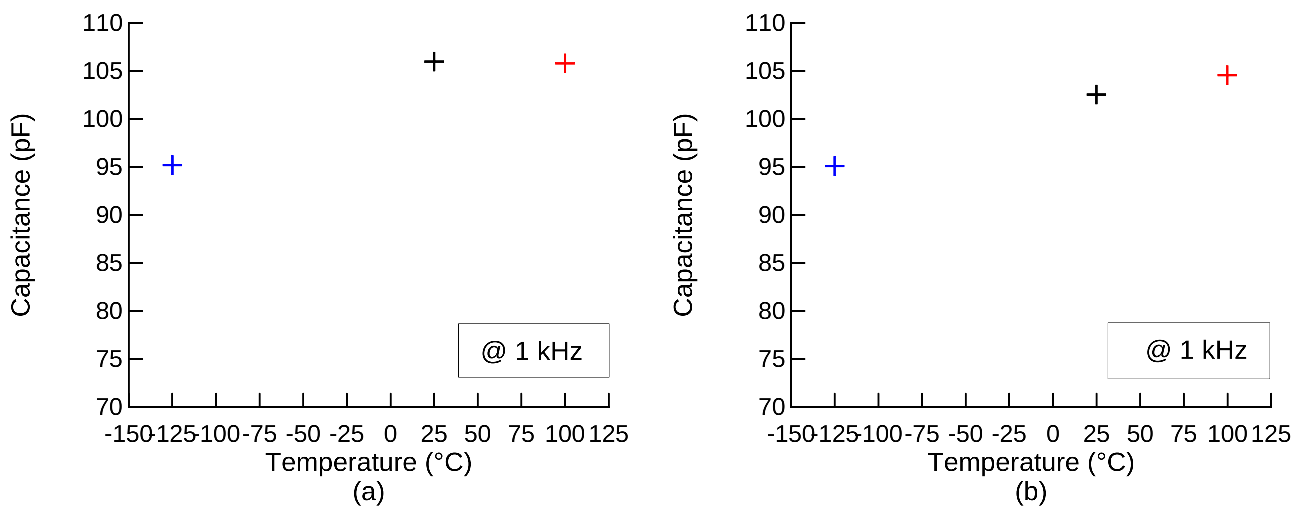

Figure 28. Capacitance versus temperature for trace 5 of board #2 during initial cycle (a), and after 4 cycles (b).

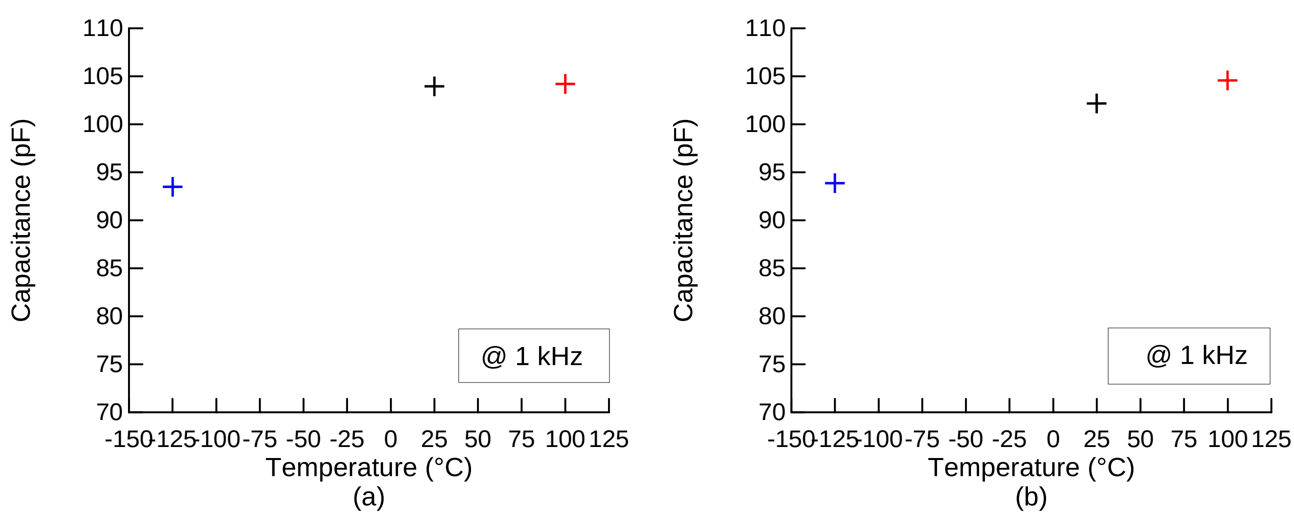

Figure 29. Capacitance versus temperature for trace 6 of board #2 during initial cycle (a), and after 4 cycles (b).

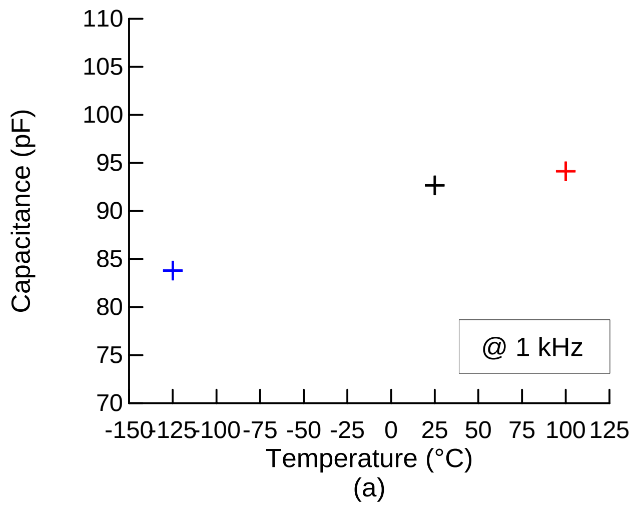

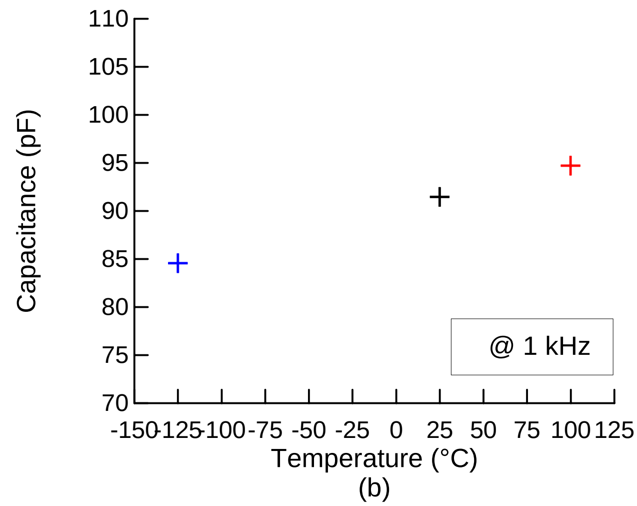

Figure 30. Capacitance versus temperature for trace 7 of board #2 during initial cycle (a), and after 4 cycles (b).

Conclusion

Two flexible printed circuit boards were characterized in terms of their dielectric properties and physical structure under thermal cycling in the temperature range between +100 °C and –125 °C. Each board had a three-layer structure of insulating material with seven serpentine-like copper traces sandwiched between them. One board had only polyimide insulation, while the other contained polyimide/boron nitride. The results obtained indicate that this limited thermal cycling produced no permanent effect on the physical integrity and the dielectric properties of either board. Only temporary changes occur in the capacitance and dissipation factor of the boards at the extreme temperatures. While the addition of boron nitride to the polyimide does not have any effect on the dielectric loss of the insulation; it tends, however, to stabilize the capacitance at high temperatures. Long term thermal cycling and aging as well as comprehensive testing are required to fully understand the behavior of these flexible printed circuit boards under multi-stress conditions to determine their suitability for use in extreme temperature environments.

Acknowledgments

This work was performed under the NASA Glenn Research Center GESS Contract # NAS3-00145 and the NASA Electronic Parts and Packaging Program (NEPP).

Appendix

Detailed experimental data obtained on the two flexible printed circuit boards are listed in this appendix. Pre-cycling, in-situ, and post-cycling measurements of the capacitance and dissipation factor in the frequency range of 200 Hz to 500 kHz are presented. Measurements of these properties during the first cycle and the last cycle of the testing sequence are also shown.

Data pertaining to the seven traces of board #1 are shown for pre-cycling, in-situ, and post-cycling conditions in Figures A1-A7 for traces 1-7, respectively. The capacitances as well as the dissipation factors under these conditions during the first cycle are depicted as a function of frequency.

Changes in the capacitance and dissipation factor for board #1 as a function of frequency during the first cycle and the 21st cycle are plotted in Figures A8-A14 for trace 1-7, respectively. Included are the measurements taken at room temperature, 100 °C and –125 °C.

Data pertaining to the seven traces of board #2 are shown for pre-cycling, in-situ, and post-cycling conditions in Figures A15-A21 for traces 1-7, respectively. The capacitances as well as the dissipation factors under these conditions during the first cycle are depicted as a function of frequency.

Changes in the capacitance and dissipation factor for board #2 as a function of frequency during the first cycle and the 4th cycle are plotted in Figures A22-A28 for trace 1-7, respectively. Included are the measurements taken at room temperature, 100 °C and –125 °C.

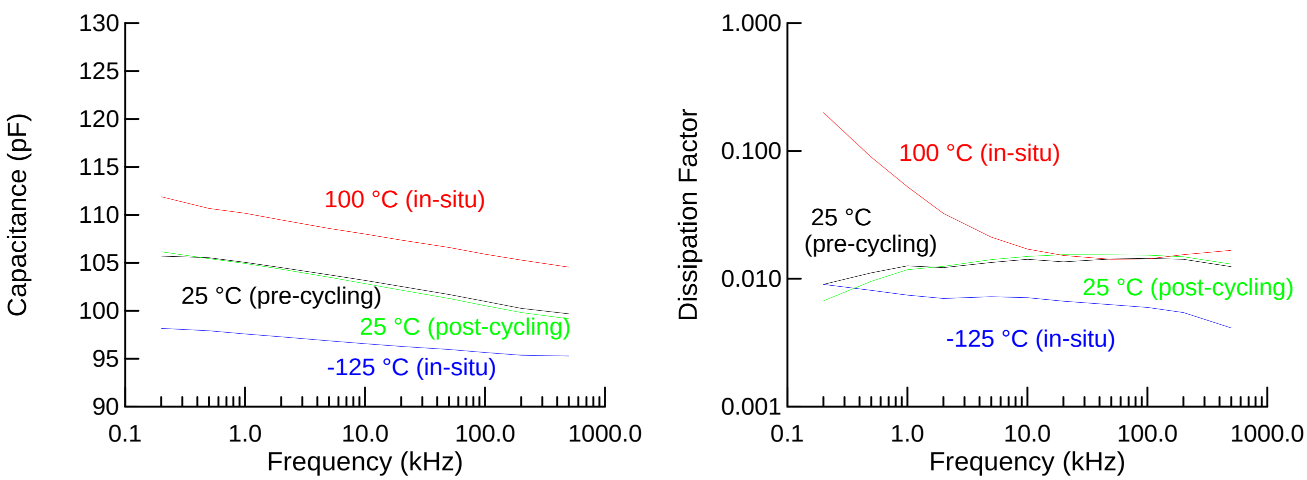

Figure A1. Capacitance and dissipation factor of trace 1 of board #1 as a function of frequency.

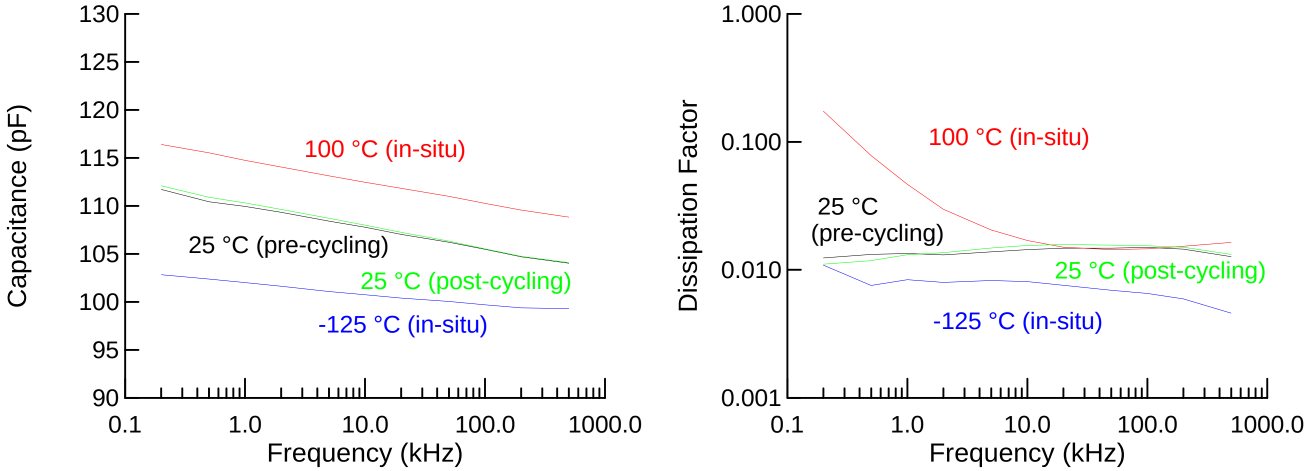

Figure A2. Capacitance and dissipation factor of trace 2 of board #1 as a function of frequency.

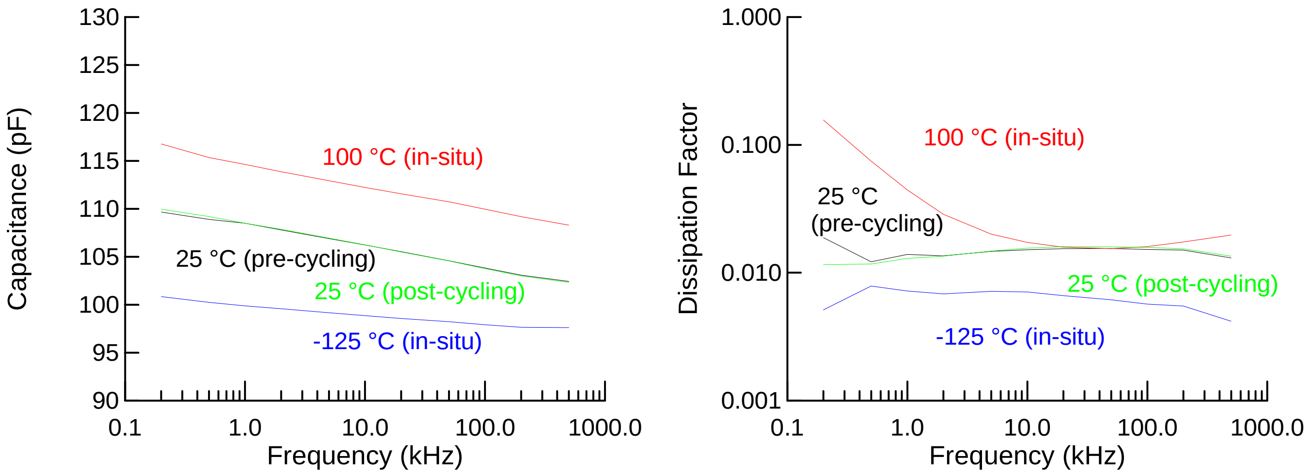

Figure A3. Capacitance and dissipation factor of trace 3 of board #1 as a function of frequency.

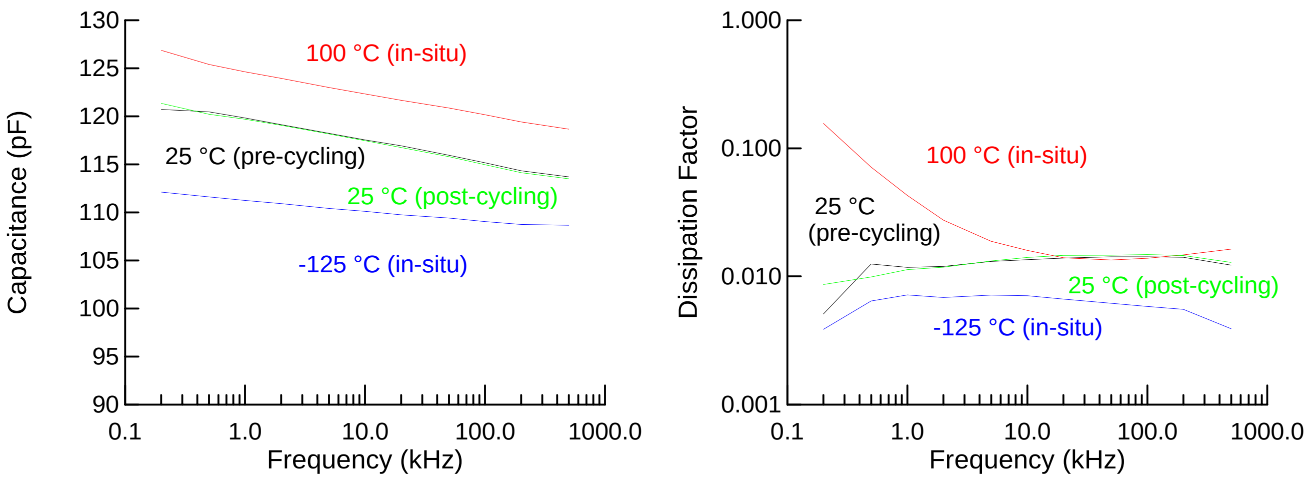

Figure A4. Capacitance and dissipation factor of trace 4 of board #1 as a function of frequency.

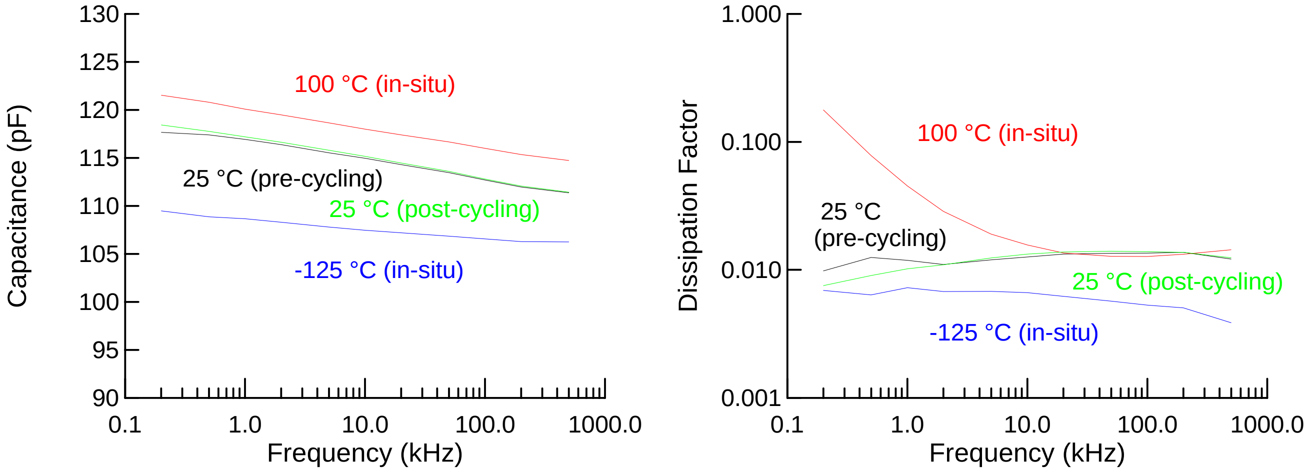

Figure A5. Capacitance and dissipation factor of trace 5 of board #1 as a function of frequency.

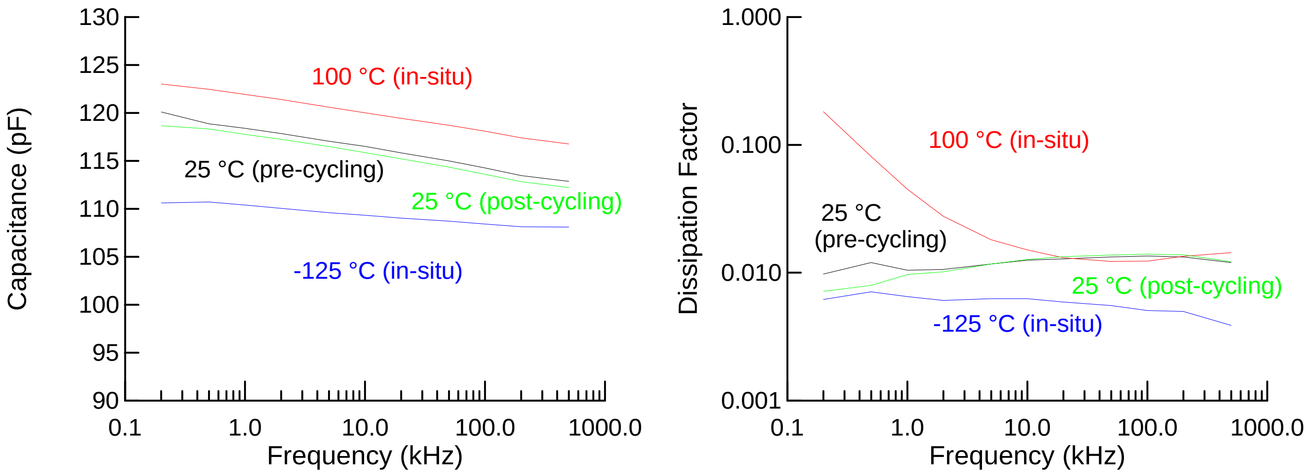

Figure A6. Capacitance and dissipation factor of trace 6 of board #1 as a function of frequency.

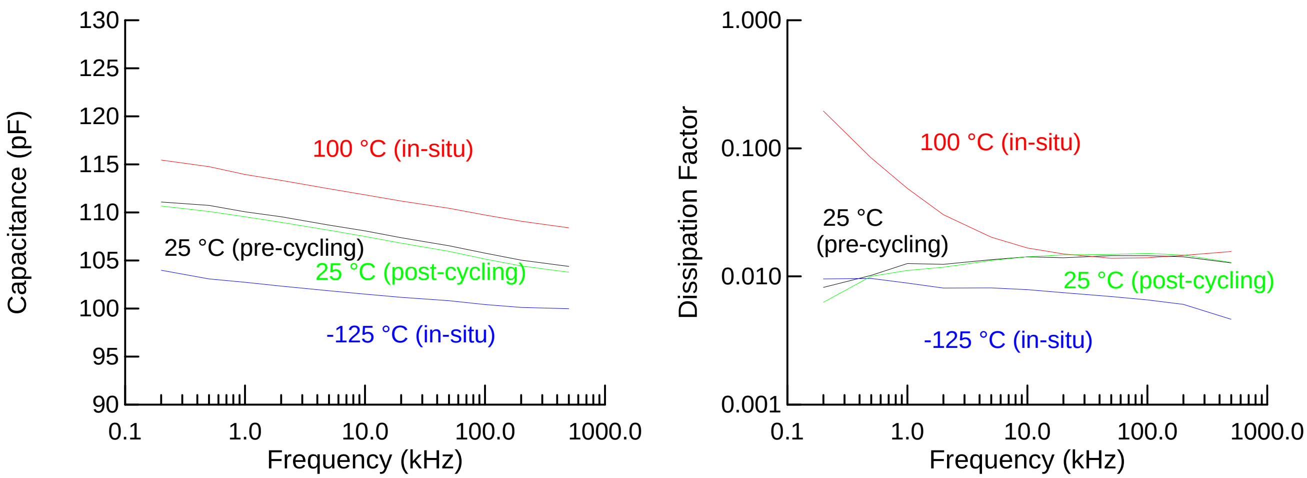

Figure A7. Capacitance and dissipation factor of trace 7 of board #1 as a function of frequency.

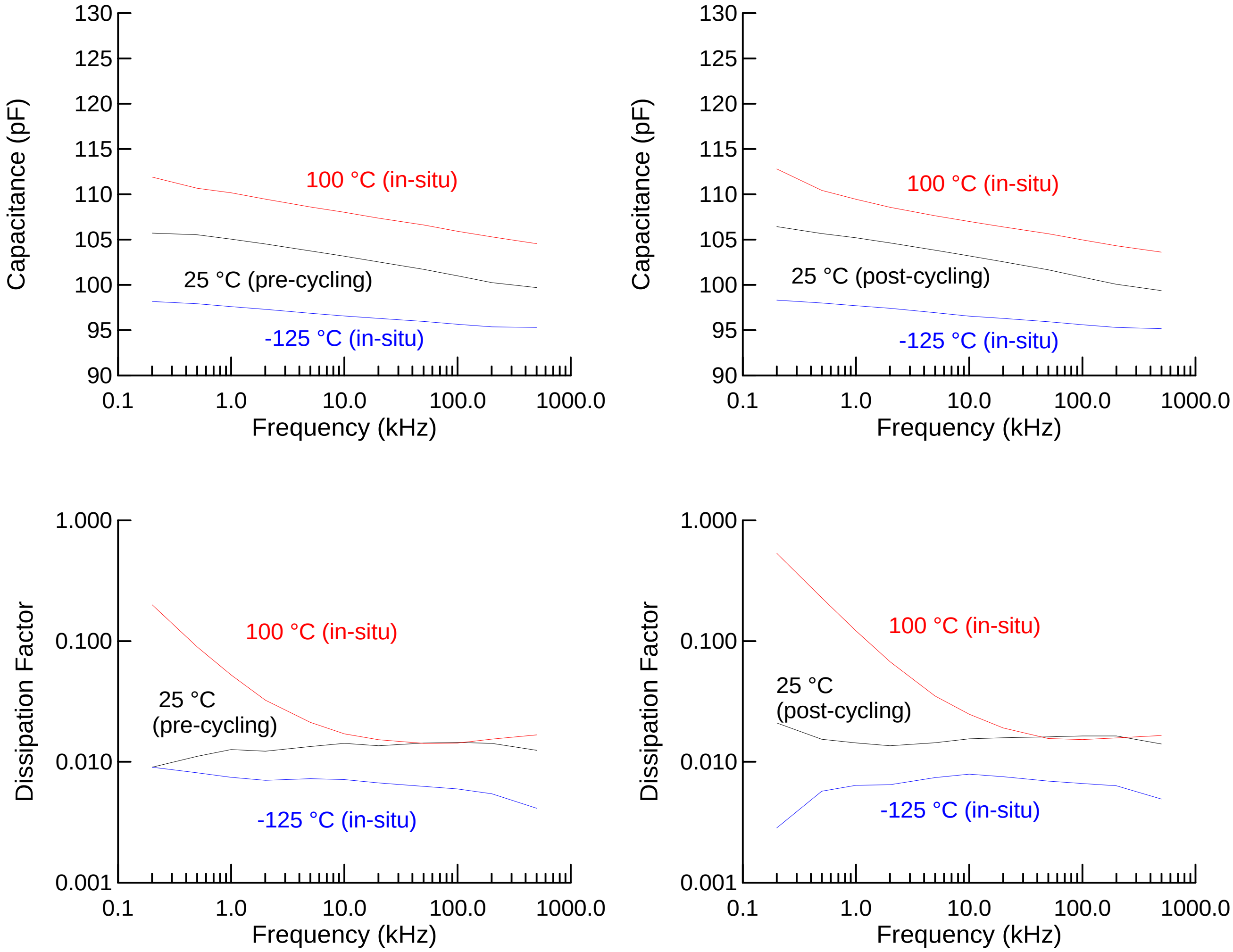

(a) (b)

Figure A8. Dielectric properties of trace 1 of board #1 during initial cycle (a), and after 21 cycles (b).

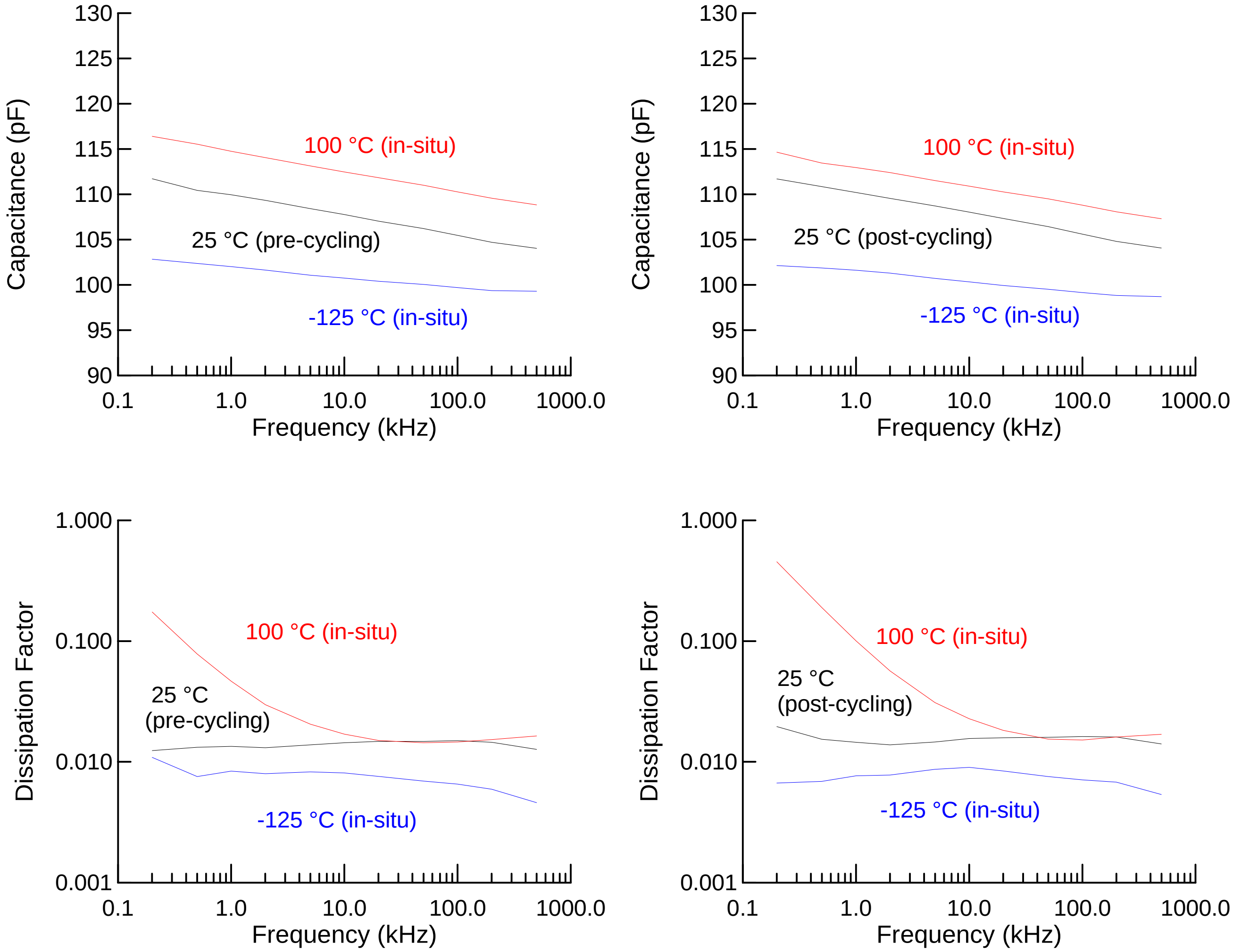

(a) (b)

Figure A9. Dielectric properties of trace 2 of board #1 during initial cycle (a), and after 21 cycles (b).

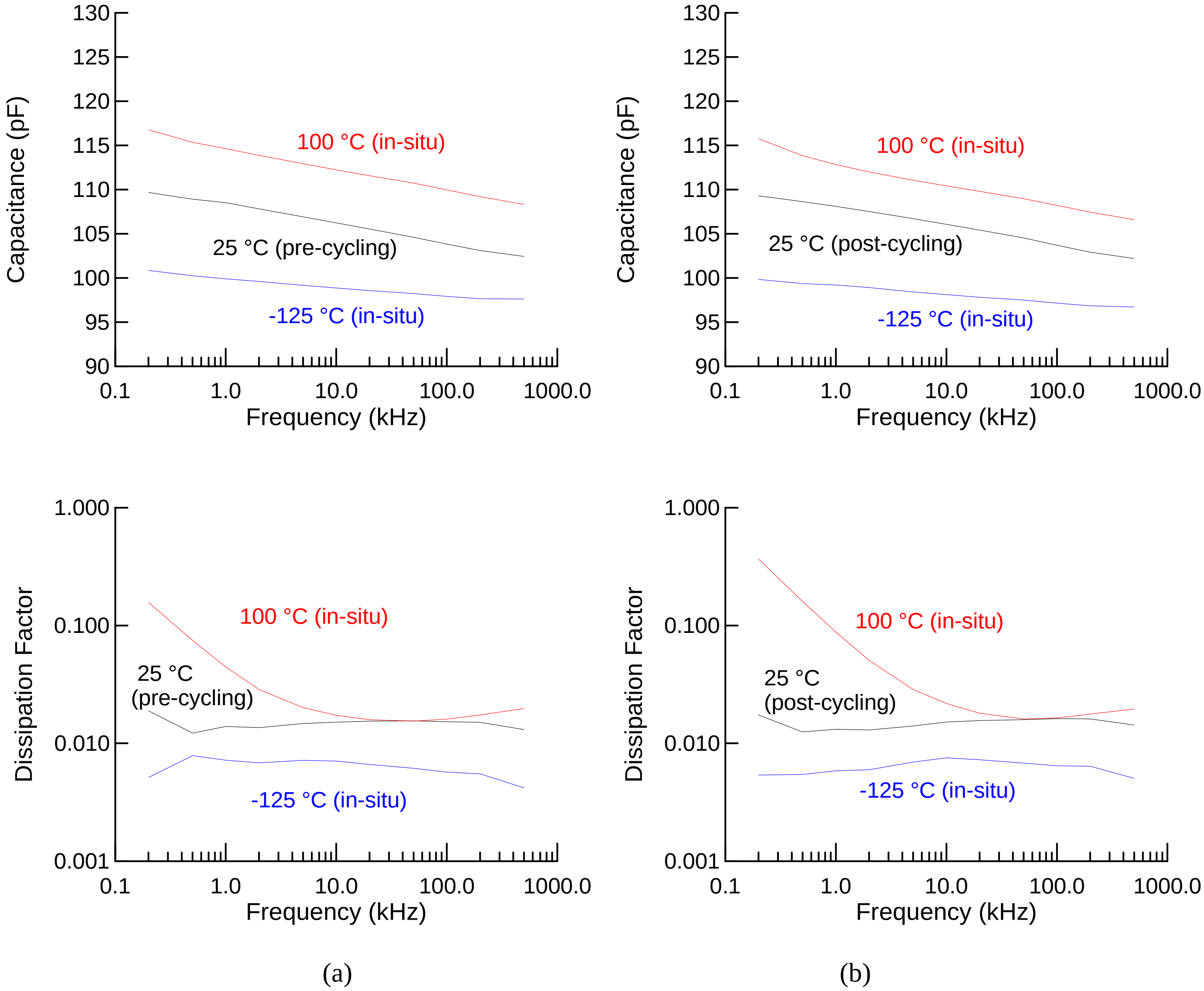

Figure A10. Dielectric properties of trace 3 of board #1 during initial cycle (a), and after 21 cycles (b).

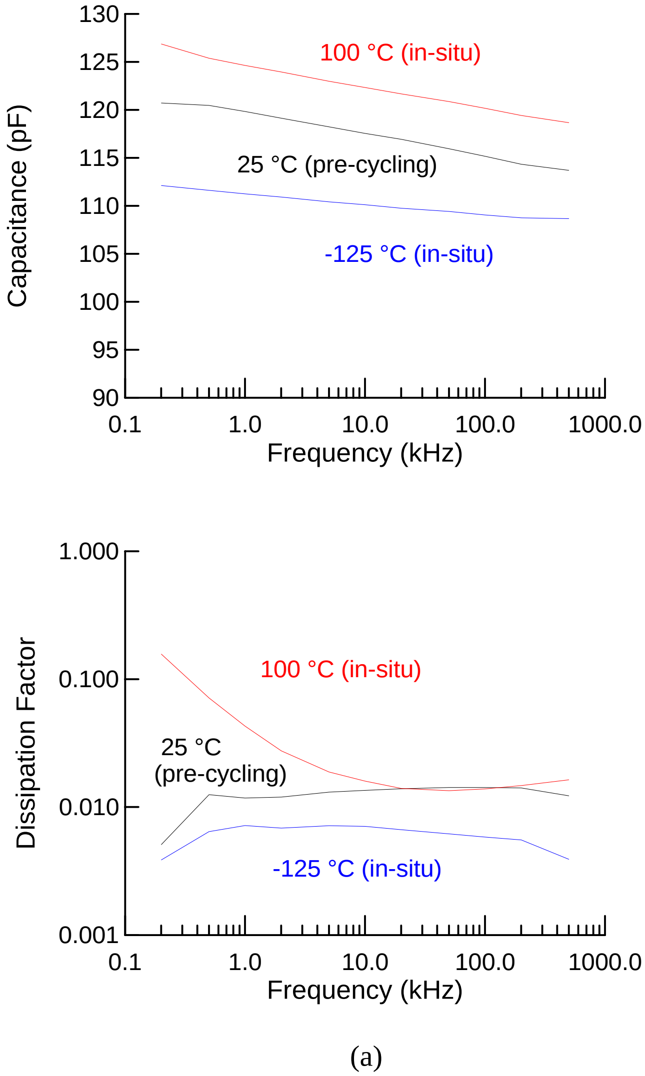

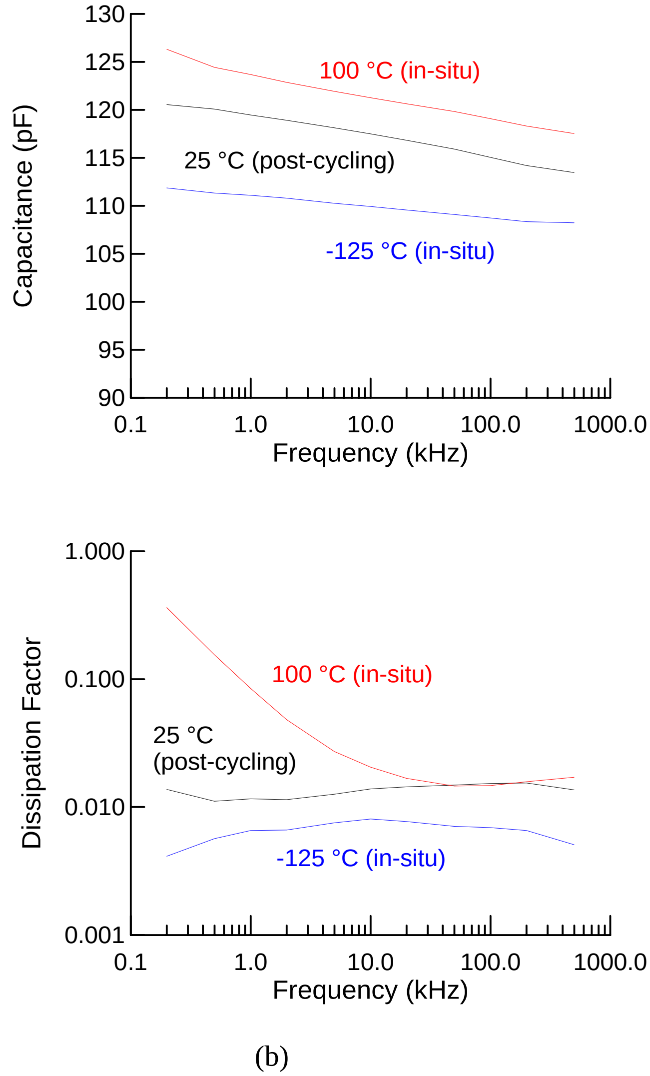

Figure A11. Dielectric properties of trace 4 of board #1 during initial cycle (a), and after 21 cycles (b).

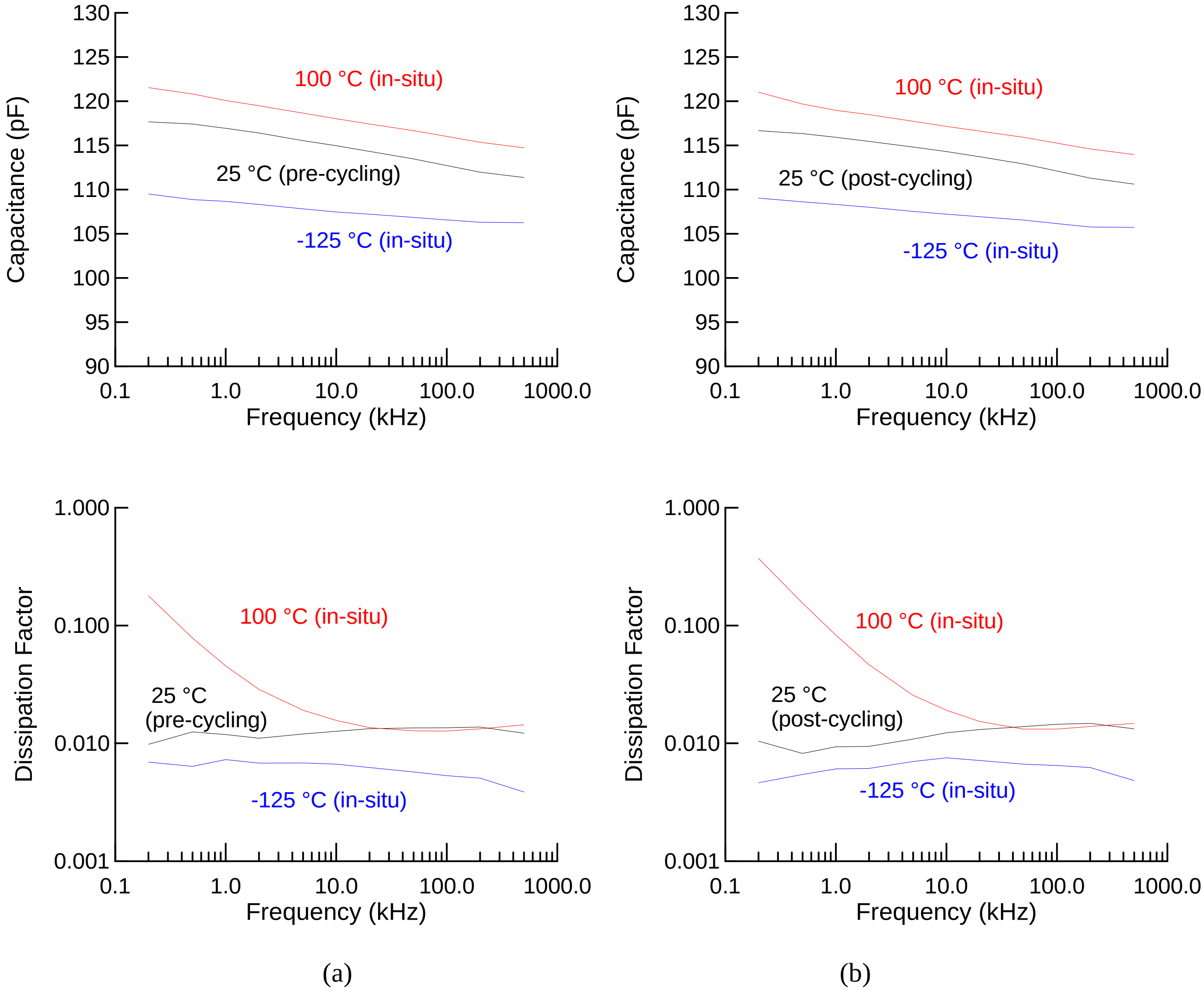

Figure A12. Dielectric properties of trace 5 of board #1 during initial cycle (a), and after 21 cycles (b).

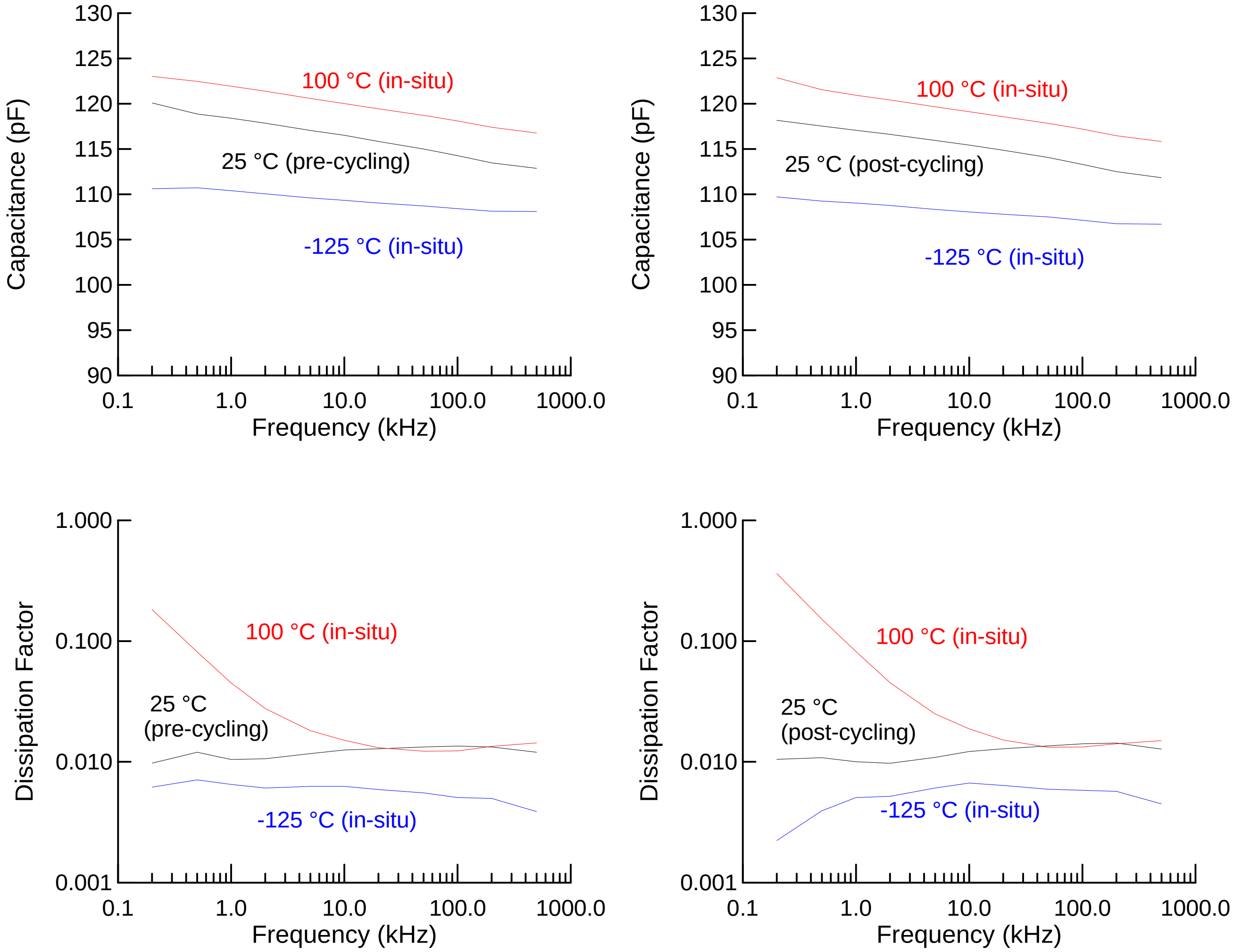

(a) (b)

Figure A13. Dielectric properties of trace 6 of board #1 during initial cycle (a), and after 21 cycles (b).

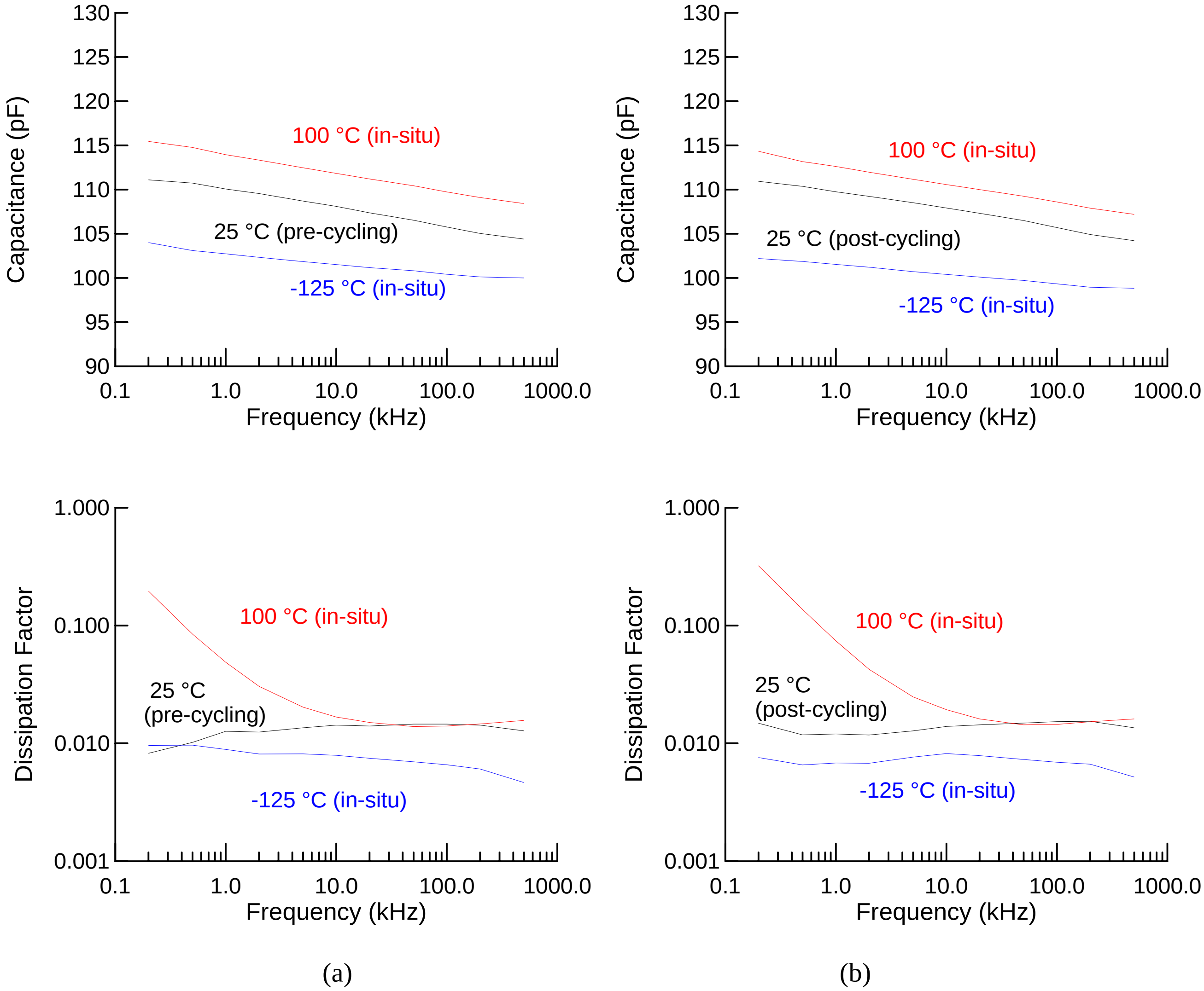

Figure A14. Dielectric properties of trace 7 of board #1 during initial cycle (a), and after 21 cycles (b).

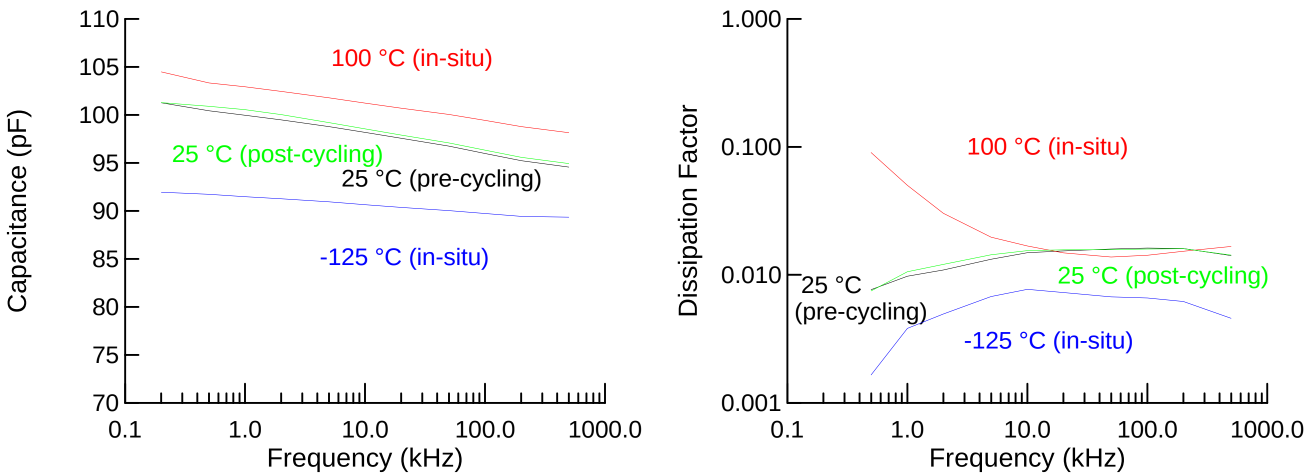

Figure A15. Capacitance and dissipation factor of trace 1 of board #2 as a function of frequency.

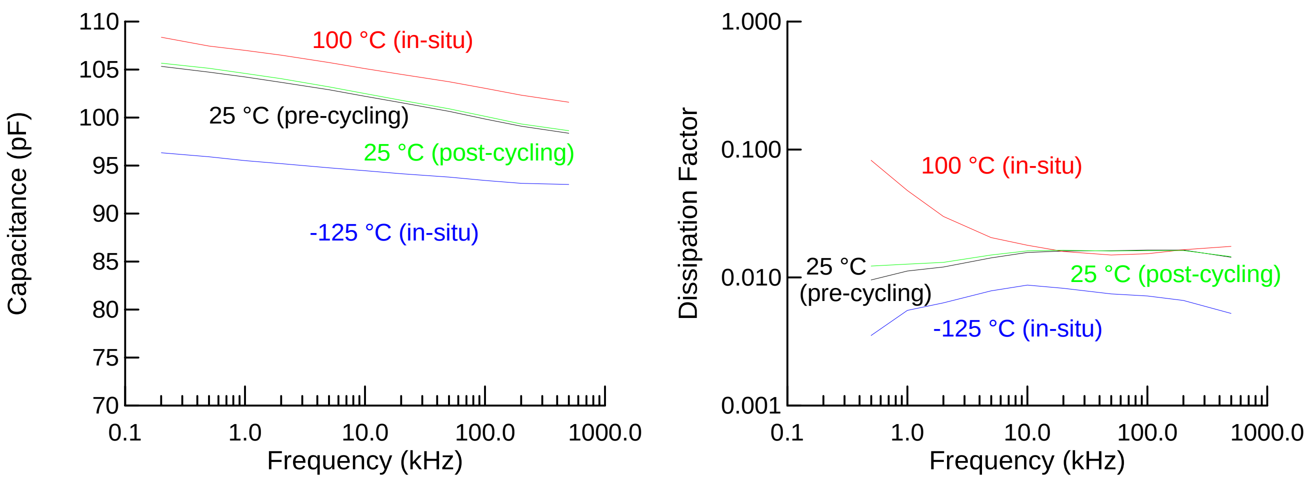

Figure A16. Capacitance and dissipation factor of trace 2 of board #2 as a function of frequency.

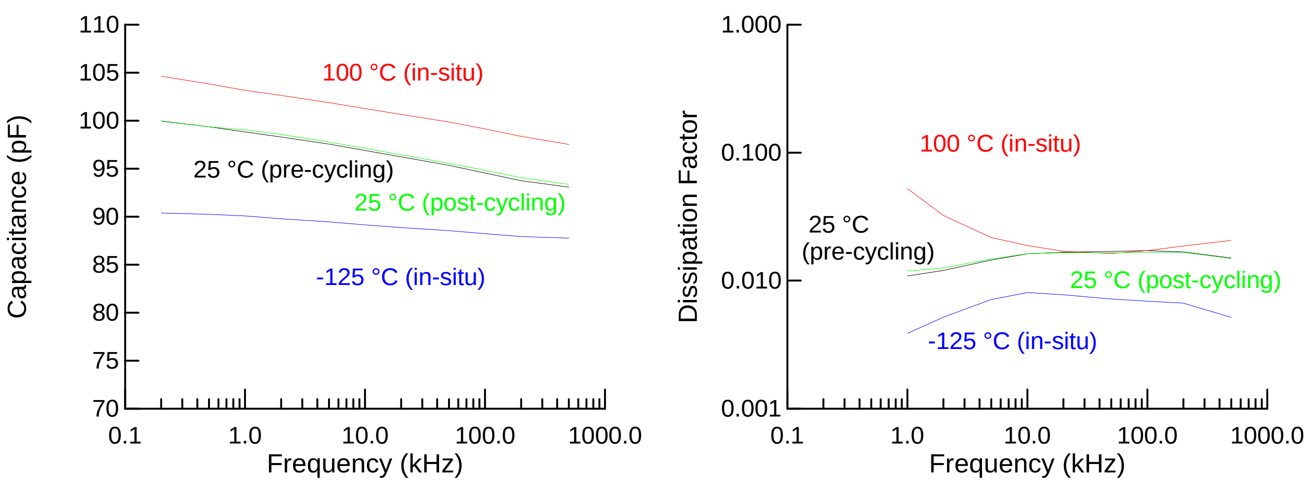

Figure A17. Capacitance and dissipation factor of trace 3 of board #2 as a function of frequency.

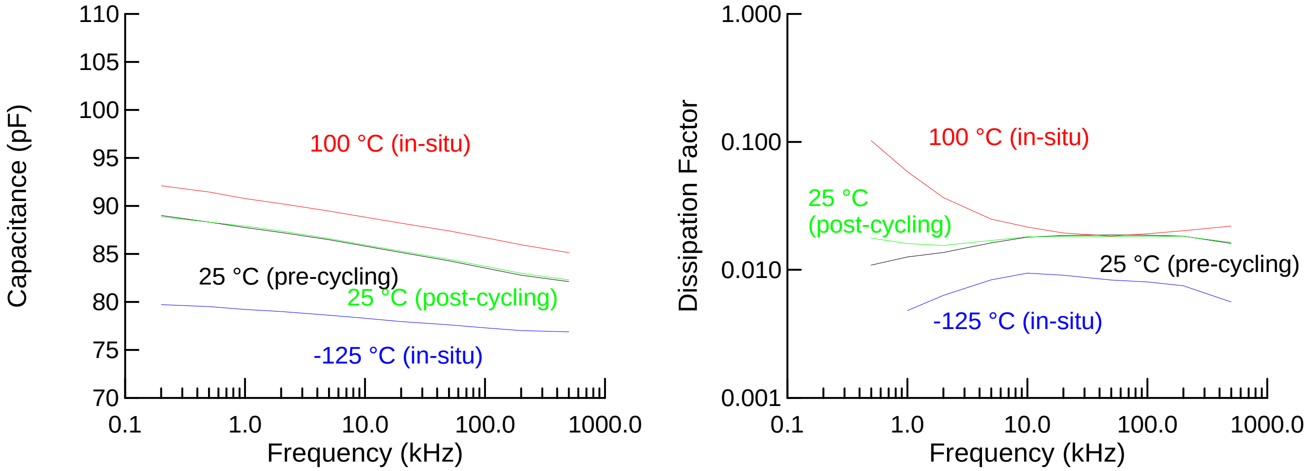

Figure A18. Capacitance and dissipation factor of trace 4 of board #2 as a function of frequency.

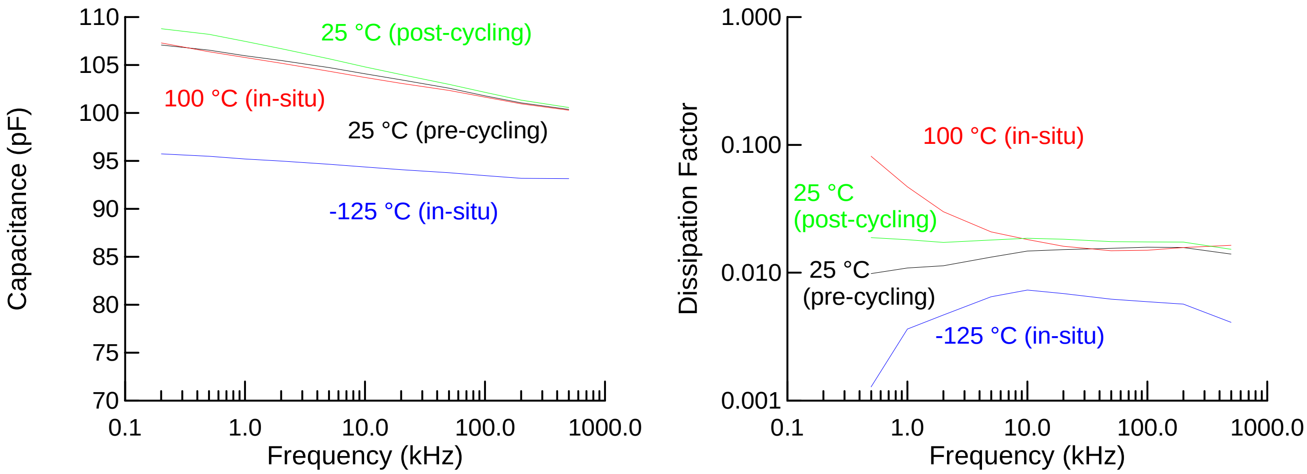

Figure A19. Capacitance and dissipation factor of trace 5 of board #2 as a function of frequency.

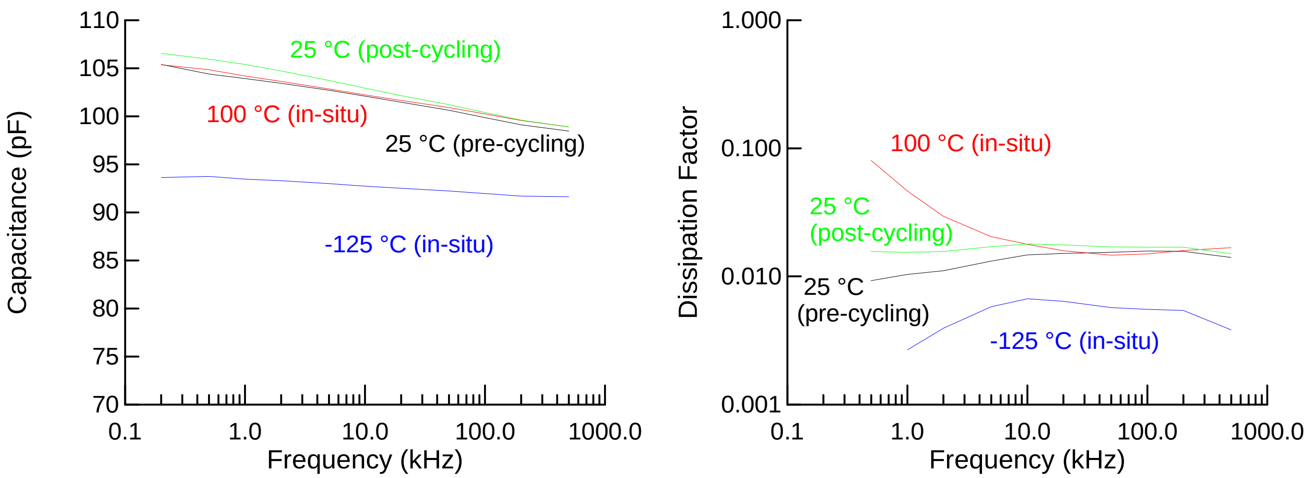

Figure A20. Capacitance and dissipation factor of trace 6 of board #2 as a function of frequency.

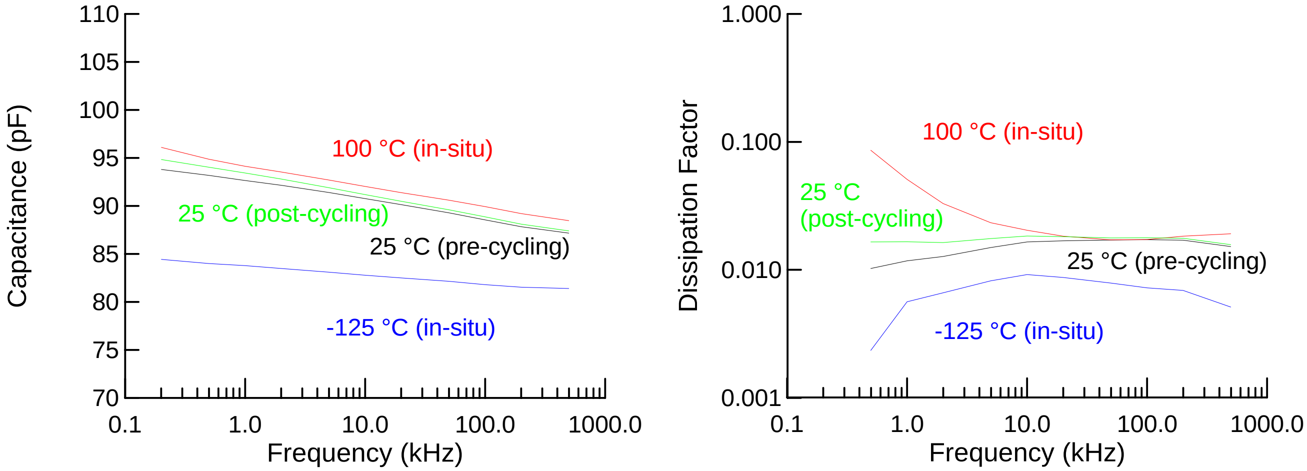

Figure A21. Capacitance and dissipation factor of trace 7 of board #2 as a function of frequency.

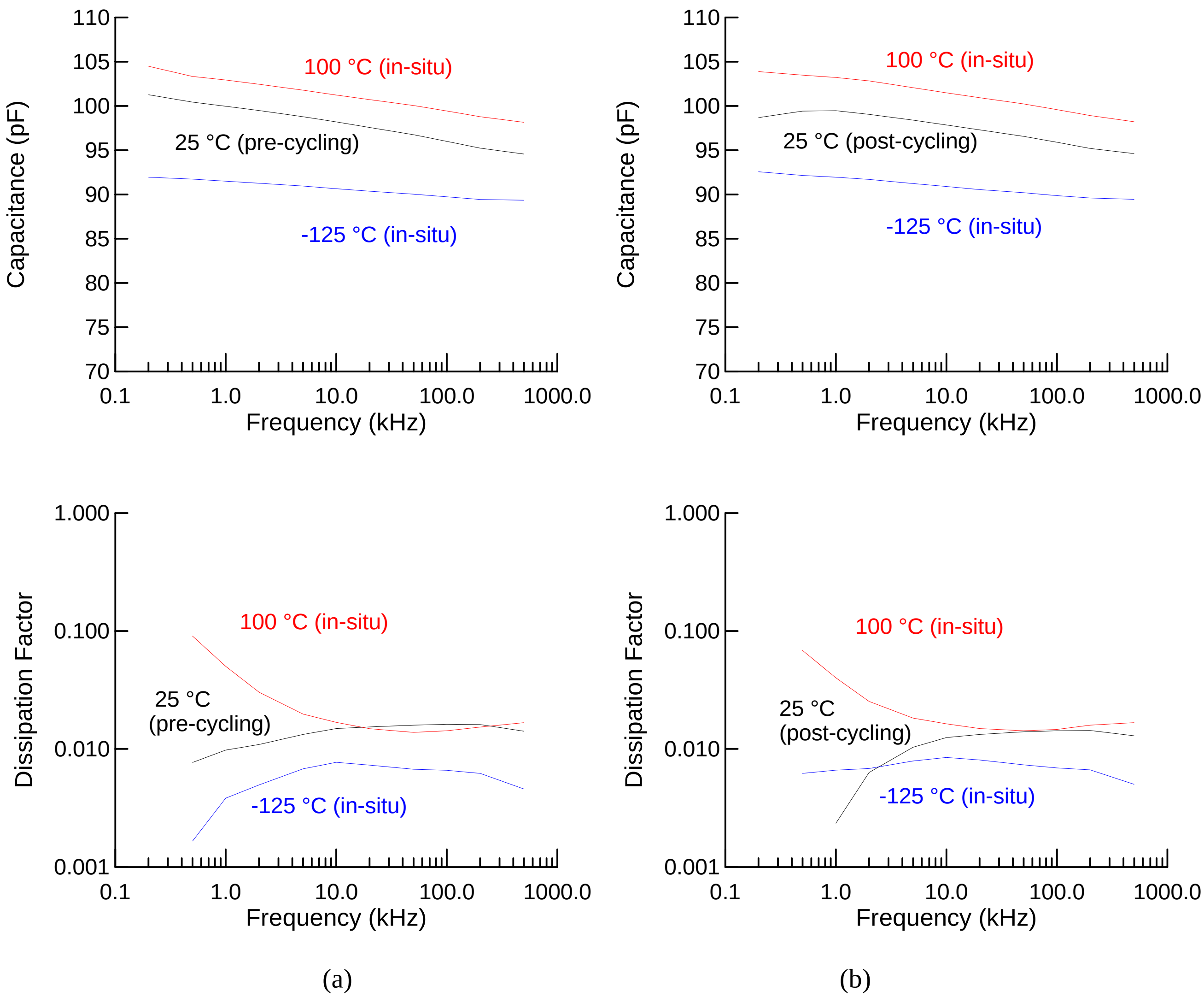

Figure A22. Dielectric properties of trace 1 of board #2 during initial cycle (a), and after 4 cycles (b).

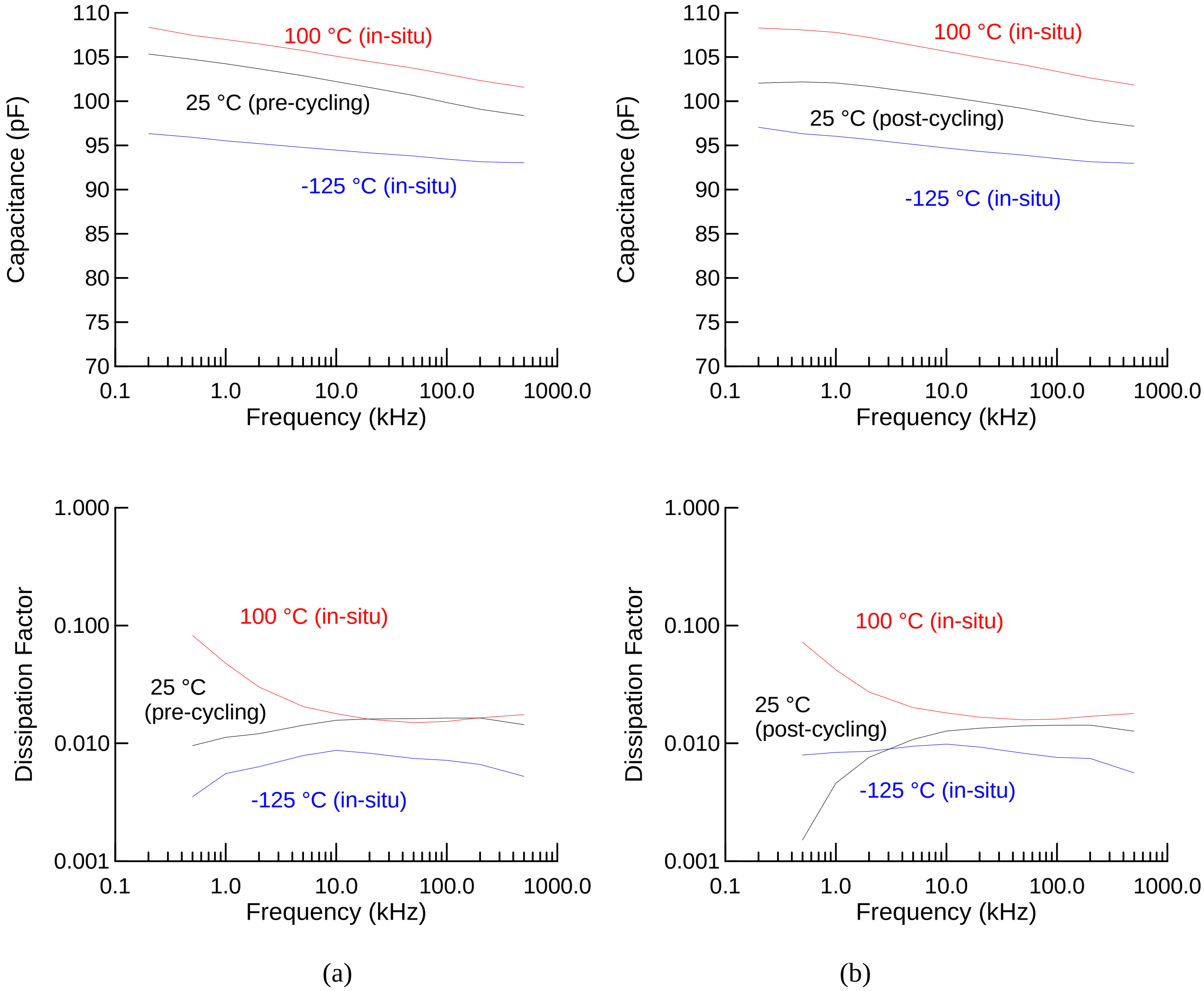

Figure A23. Dielectric properties of trace 2 of board #2 during initial cycle (a), and after 4 cycles (b).

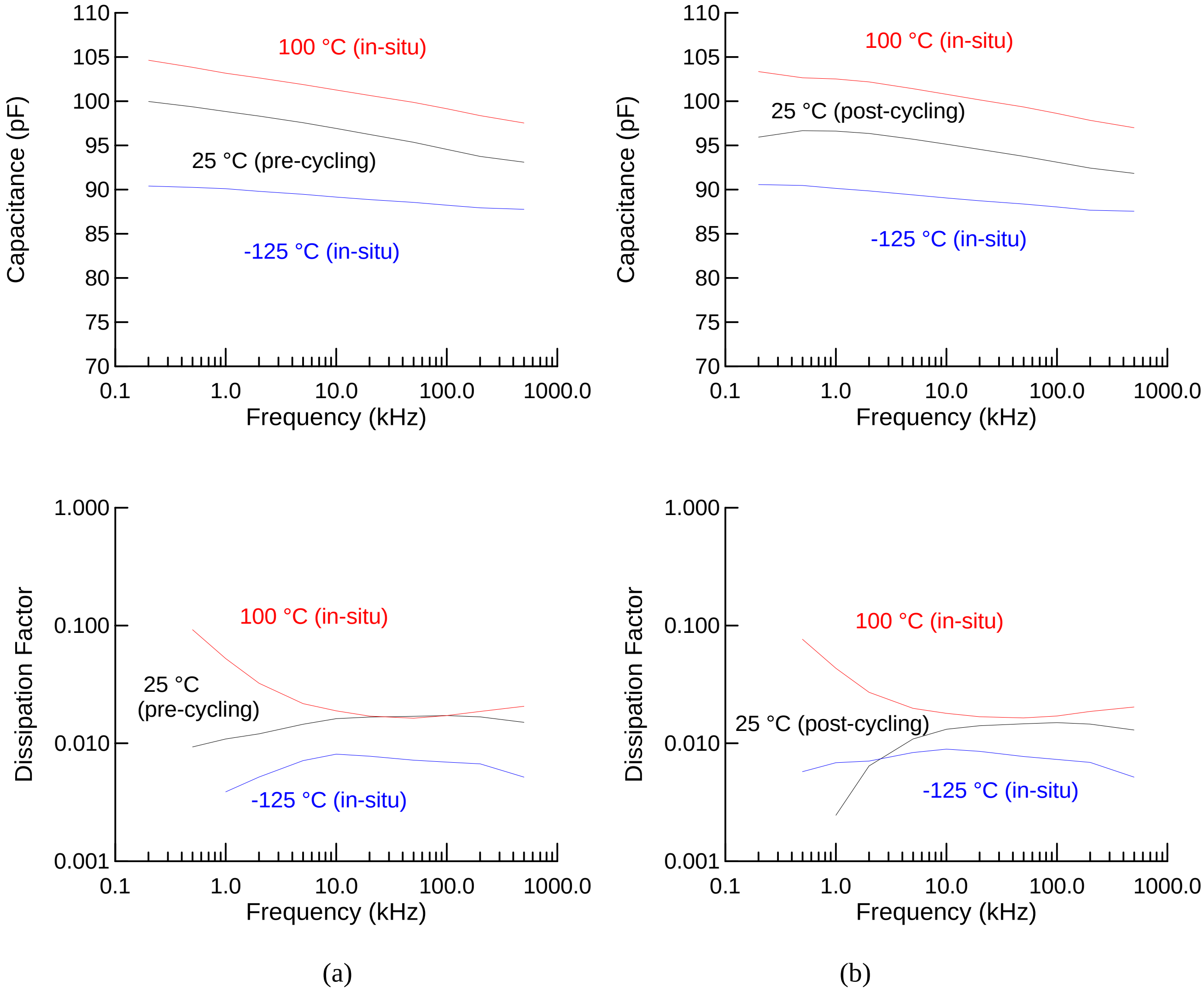

Figure A24. Dielectric properties of trace 3 of board #2 during initial cycle (a), and after 4 cycles (b).

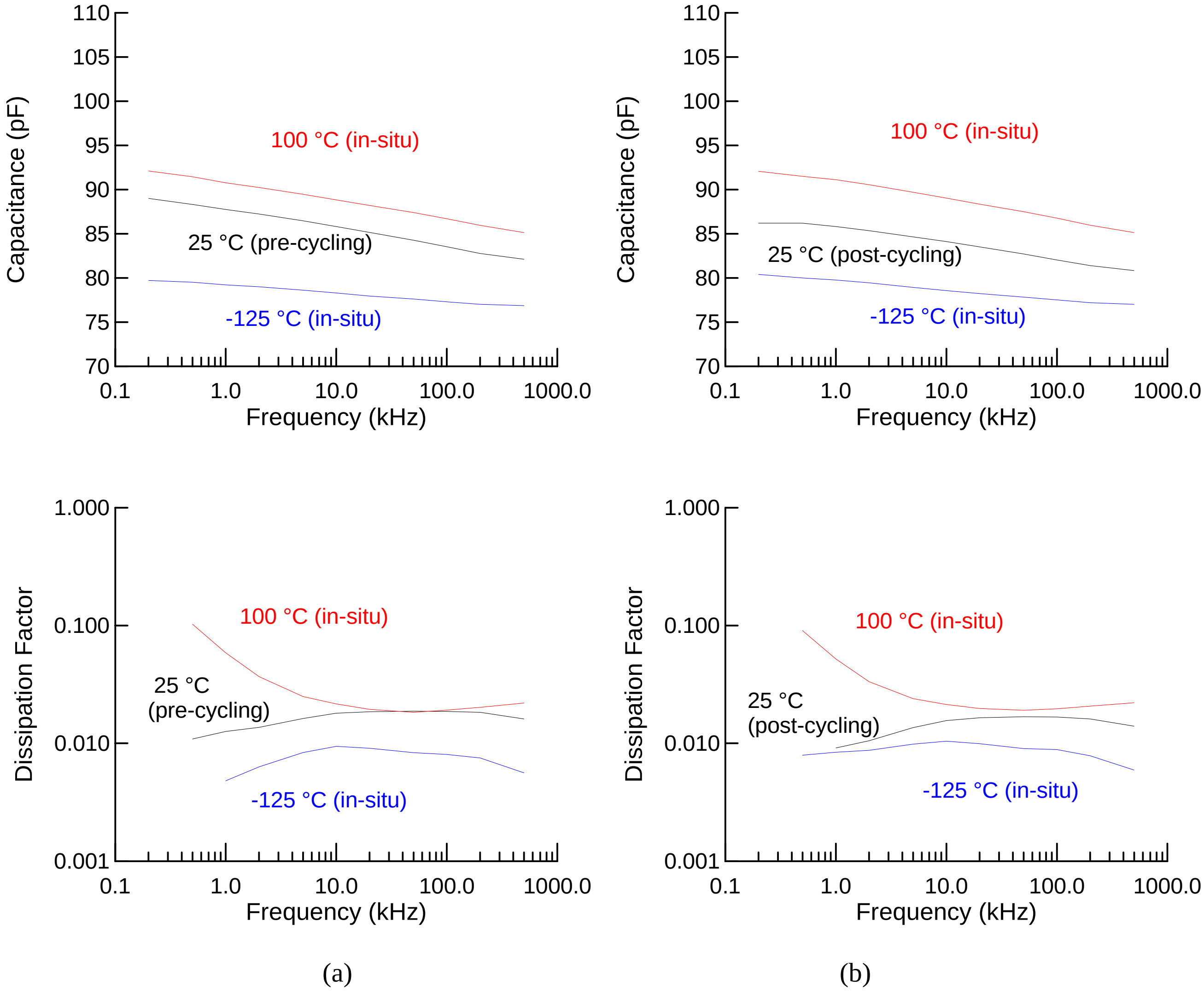

Figure A25. Dielectric properties of trace 4 of board #2 during initial cycle (a), and after 4 cycles (b).

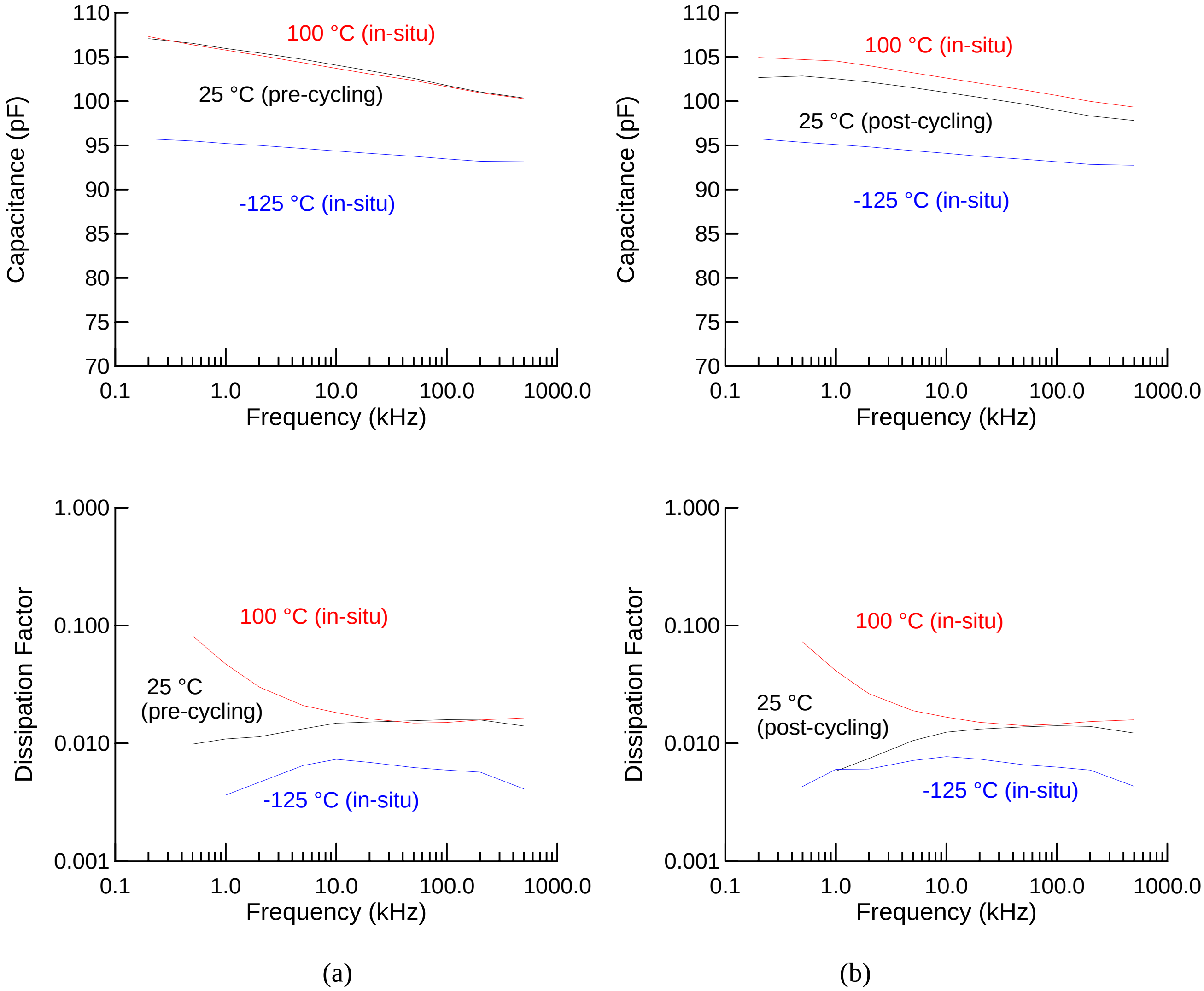

Figure A26. Dielectric properties of trace 5 of board #2 during initial cycle (a), and after 4 cycles (b).

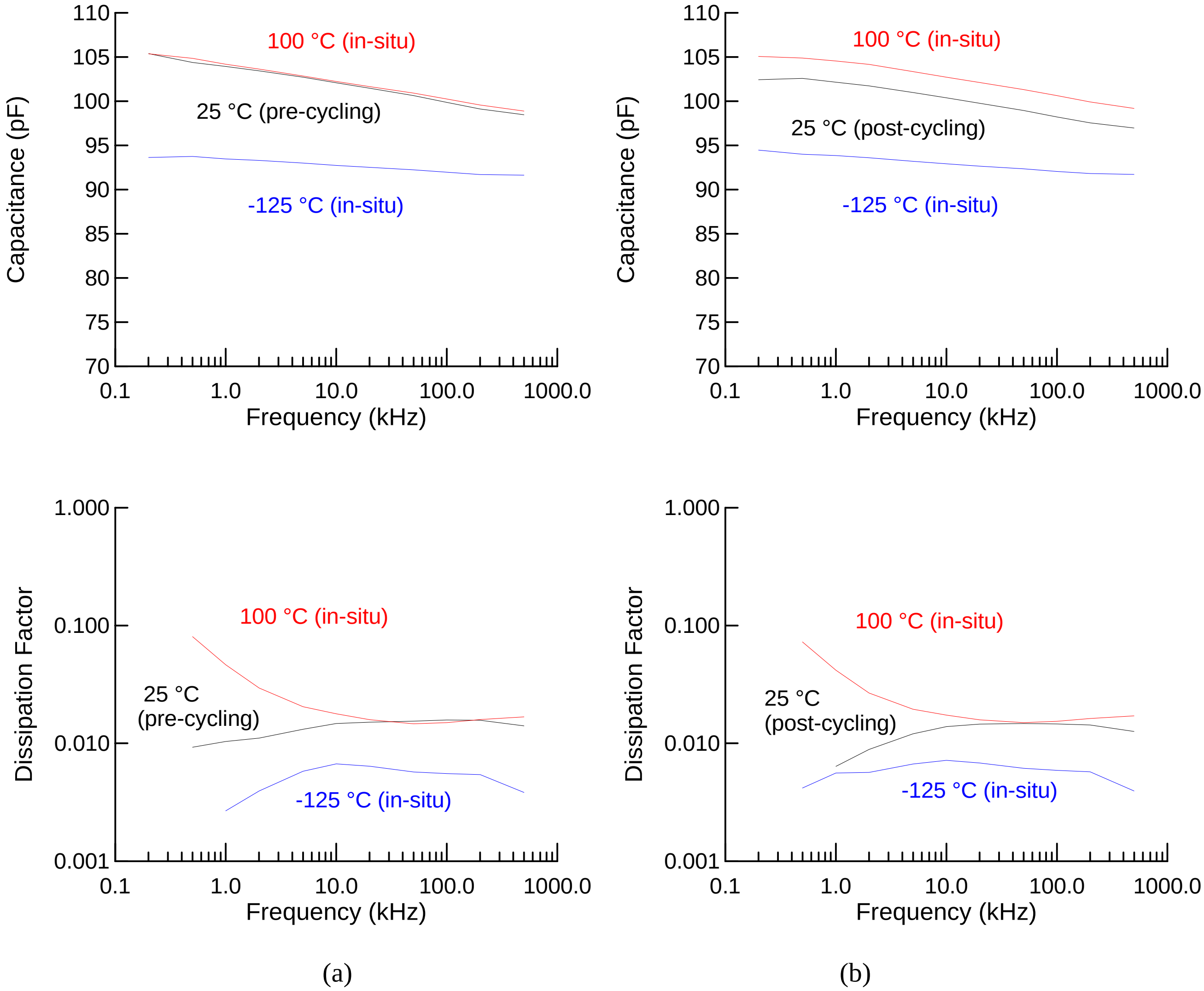

Figure A27. Dielectric properties of trace 6 of board #2 during initial cycle (a), and after 4 cycles (b).

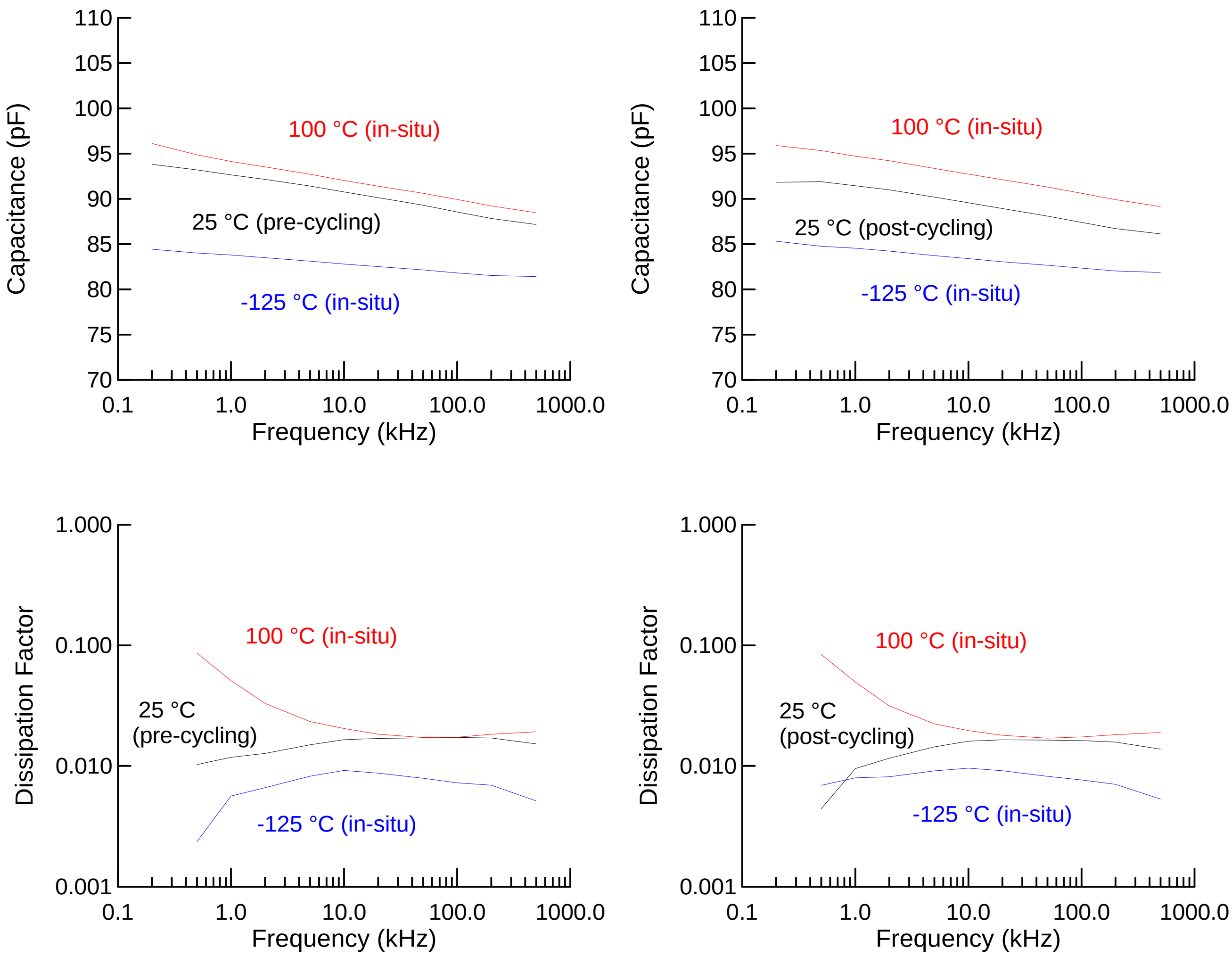

(a) (b)

Figure A28. Dielectric properties of trace 7 of board #2 during initial cycle (a), and after 4 cycles (b).